University of Massachusetts Amherst
ScholarWorks@UMass Amherst

Doctoral Dissertations 1896 - February 2014

1-1-1976

On white dwarf models of variable compact x-ray sources.

Paul Donald Guthrie
University of Massachusetts Amherst

Follow this and additional works at: https://scholarworks.umass.edu/dissertations_1

Recommended Citation

Guthrie, Paul Donald, "On white dwarf models of variable compact x-ray sources." (1976). *Doctoral Dissertations 1896 - February 2014*. 1737.
https://scholarworks.umass.edu/dissertations_1/1737

This Open Access Dissertation is brought to you for free and open access by ScholarWorks@UMass Amherst. It has been accepted for inclusion in Doctoral Dissertations 1896 - February 2014 by an authorized administrator of ScholarWorks@UMass Amherst. For more information, please contact scholarworks@library.umass.edu.

312066 0015 4648 3

ON WHITE DWARF MODELS OF VARIABLE COMPACT X-RAY SOURCES

A Dissertation Presented

By

Paul Donald Guthrie

Submitted to the Graduate School of the
University of Massachusetts in partial
fulfillment of the requirements for the degree of

DOCTOR OF PHILOSOPHY

November 1976

Astronomy

ⓒ Paul Donald Guthrie 1976

All Rights Reserved

ON WHITE DWARF MODELS OF VARIABLE COMPACT X-RAY SOURCES

A Dissertation

By

Paul Donald Guthrie

Approved as to style and content by:

Eugene H. Tademaru

Eugene H. Tademaru, Chairman of Committee

William M. Irvine

William M. Irvine, Member

George Greenstein, Member

James Walker

James Walker, Member

F. W. Byron, Jr.

Frederick W. Byron, Jr., Department Head
Department of Physics and Astronomy

November 1976

ACKNOWLEDGEMENTS

No dissertation is due solely to the efforts of the author. I am particularly grateful to my advisor, Professor Eugene Tademaru, for the many discussions and insights which helped convert confusion into understanding. I would also like to thank my fellow graduate students, especially Larry Esposito, John Bally and Robin Waldron, for listening and offering helpful suggestions. Ms. Terri Grzybowski has cheerfully endured the changes and corrections in typing the drafts and the final manuscript.

Finally, for loving faith and support in moments of the greatest frustration and discouragement, I am indebted to my wife Betsy.

ABSTRACT

On White Dwarf Models of Variable Compact X-Ray Sources

(February 1977)

Paul D. Guthrie, B.A., Cornell University
M.S., University of Massachusetts, Ph.D.,
University of Massachusetts

Directed by: Professor Eugene Tademaru

It is known that white dwarfs exist in some binary systems which undergo Roche lobe mass transfer during their evolution. Nova theory indicates that these white dwarfs can develop a runaway thermonuclear reaction in the non-degenerate hydrogen shell, thus ejecting the outer layers of the star, although not necessarily to escape velocity. When this occurs during periods of high mass transfer the system must become an x-ray source. Since the radiation will be produced by free-free emission in a shock, the luminosity will vary as the shock velocity changes.

An expression for the opacity-limited luminosity is developed, giving luminosities of less than 10^{37} erg s^{-1}. It is argued that a model involving a detached shell will produce periods of nuclear burning with the intensity controlled by the net loss or gain of kinetic energy of the shell to or from the accreting gas. This implies an equilibrium state of the system defined by balancing the energy gains and losses by the shell during one cycle of radial motion.

A method is developed for computing the luminosity and spectrum of the x-ray emission from the shocked gas at a given shock velocity.

The equation of motion of the shell is developed. Two asymptotic limits are defined; that in which gravity dominates and that in which the ram pressure dominates. These are solved analytically and the general equation of motion is solved numerically. Equilibrium conditions are obtained for the analytic solutions.

Combining the velocity solutions and the radiation analysis, the luminosity is obtained as a function of time for the limiting cases and for intermediate cases where the general equation of motion is used. These light curves are developed for various combinations of the parameters describing the detonation conditions and the accretion flow conditions. The time behavior of the spectrum is obtained for several cases. It is found that this is characteristic for models of this type and distinct from the spectral time development predicted by other types of models for x-ray sources.

It is concluded that some white dwarfs in binaries should undergo subnova detonations during accretion, and should thus become x-ray sources. Such sources should be identifiable by their spectral time behavior and comparison of their light curves with model predictions should offer insight into the underlying source conditions. The predictions are compared with existing observations of x-ray sources.

TABLE OF CONTENTS

Page

Acknowledgements i

Abstract ii

Chapter I: Introduction 1

Chapter II: General Characteristics and Constraints 9

  §1. Introduction 9

  §2. Observational Constraints 10

  §3. Opacity Limits 11

  §4. Equilibrium and Stability 13

Chapter III: Radiation Analysis 19

Chapter IV: Velocity of the Shock 27

  §1. Acceleration 27

    a) Radiation pressure 27

    b) Emergent shock 27

  §2. Decay 32

    a) The QSP limit 32

    b) The gravitational limit 32

Chapter V: QSP Equation of Motion 45

  §1. Solution 45

  §2. Stability 51

  §3. Summary 58

Chapter VI: Light Curves and Spectra 61

Chapter VII: Discussion and Conclusion 74

References 85

FIGURE CAPTIONS

Page

Figure 3-1a: Run of temperature, bulk velocity and density relative to initial values in cooling layer of radiative shock at shock velocity $v_s = 3 \times 10^8$ cm s^{-1}, $\rho_a = 10^{-8}$ g cm^{-3}. 24

Figure 3-1b: Run of temperature, bulk velocity and density relative to initial values in cooling layer of radiative shock at shock velocity $v_s = 6 \times 10^8$ cm s^{-1}, $\rho_a = 10^{-8}$ g cm^{-3}. 24

Figure 3-2: Computed spectrum and spectrum of homogeneous region at $T = 10^8$ K. 26

Figure 4-1: Solution to QSP equation of motion for
$M_o = 20$ g cm^{-2}
$V_o = 1.5 \times 10^8$ cm s^{-1}
$\rho_a = 10^{-9}$ g cm^{-3}
$M_* = .5\ M_\odot$. 41

Figure 4-2: Solution to QSP equation of motion for
$M_o = 20$ g cm^{-2}
$V_o = 3 \times 10^7$ cm s^{-1}
$\rho_a = 10^{-9}$ g cm^{-3}
$M_* = .5\ M_\odot$. 42

Page

Figure 4-3: Velocity solutions to general equation of motion (4.7) for

$V_o = 3 \times 10^8$ cm s^{-1}

$\rho_a = 10^{-9}$ g cm^{-7}

$M_* = .5\ M_\odot$

M_o as labeled. 43

Figure 4-4: Position (height) solutions to general equation of motion (4.7) as in Figure 4-3. 44

Figure 5-1: Impact mass in units of initial shell mass as a function of initial velocity for given accretion velocity $v_a (\alpha \equiv [2 \frac{v_o + v_a}{v_a} - 1]^{1/2})$. 49

Figure 5-2: Ratio of shell kinetic energy at impact to initial value as a function of initial velocity. ... 52

Figure 5-3: Equilibrium period in units of μ_o as a function of the initial velocity parameter α. 56

Figure 5-4: The function $G(\alpha)$. 59

Figure 6-1: Light curves for the general Equation (4.7) with $V_o = 3 \times 10^8$ cm s^{-1} and various values of M_o. Stellar mass is $.5\ M_\odot$ and $\rho = 10^{-9}$ g cm^{-3}. 63

Figure 6-2: Light curves for the general equation with $M_o = 20$ g cm^{-2} and various values of V_o.

Page

Same stellar and accretion parameters as in 6-1. 64

Figure 6-3: Gravitational limit light curves for various values of V_o and stellar mass .5 $M_\odot$. 65

Figure 6-4: QSP limit light curves for $v_a = 3 \times 10^8$ cm s^{-1}, $V_o = 3 \times 10^8$ cm s^{-1} and various values of M_o. 66

Figure 6-5: QSP limit light curves for $v_a = 3 \times 10^8$ cm s^{-1}, $M_o = 20$ g cm^{-2} and various values of V_o. 67

Figure 6-6: Same as Figure 6-5 on a semi-log scale illustrating the shape of the decay phase. 69

Figure 6-7: Same as Figure 6-3 on a semi-log scale illustrating the shape of the decay phase. 70

Figure 6-8: Hardness ratio vs. time. 72

Figure 6-9: Luminosity per unit area as a general function of the relative velocity v for two values of the accretion density, ρ. 73

Figure 7-1: Loss ratio R_L as a function of radiation temperature for various plasma conditions. 82

CHAPTER I

INTRODUCTION

This work concerns most aspects of a particular model for variable compact x-ray sources, based on a pulsating white dwarf. As we will consider later whether this type of model behaves like any of the observed x-ray sources, the presentation of the model is here prefaced with a short summary of the characteristics of compact x-ray sources. One of the striking features of this class of objects is the preponderance of binary systems. This strongly supports theories in which matter is lost by a star in its giant phase and accretes onto a binary companion, providing a simple energy source for the emission of x-rays. Although not all compact x-ray sources are known to be in binaries, there is no such source at this point for which accretion can be ruled out.

The time behavior of these sources can be grouped into three classes: 1) pulsed sources, 2) transient sources, and 3) burst sources. Each class is characterized in terms of the characteristic time scales of variations in the x-ray flux, and the regularity of those variations.

The first class, the pulsed sources, contains only two members, Her X-1 and Cen X-3. They are characterized by a highly regular periodic modulation of the x-ray flux with periods of the order of seconds. There are also other modulations at longer periods, but these are not necessarily intrinsic to the x-ray source (e.g. eclipses). The rapid pulsations clearly require a model with a rather regular clock. Many authors take this to indicate the presence of a rotating neutron star. However the shortest known period, ~ 1.2 s for Her X-1, is barely tolerable for a whole-body vibration of a white dwarf without destroying the star. If only a fraction of the star, such as an outer shell, is participating in the vibration the periods are quite tolerable. Although there are major problems involved in applying the white dwarf model developed in this work to either of the known pulsed sources, it will be shown that in principle the model can produce such behavior.

The second observed class is that of the transient sources. These sources "turn on"; they go from below detector limits to fluxes comparable to the brightest known steady sources and then disappear again, all on a time scale of the order of weeks. At least two are known to be pulsed during their observed existence, but the periods involved are on the order of hundreds of seconds, much longer than the pulse periods in class one. The paucity of observations makes comparison with detailed model predictions rather inconclusive for this class. However, the transient behavior, combined with at least some cases of pulsation, is suggestive of variations in the accretion rate rather than processes intrinsic to the x-ray source itself.

The third, and newest, class is that of the burst sources. These are characterized by "bursts" of x-ray emission which rise very rapidly and then decay more or less exponentially. The time constant for this decay is variable both within and between sources, but is on the order of a few seconds (Clark et al. 1976). In some cases the bursts are quasi-periodic, but with a large jitter. The time scales for the intervals between bursts range from tenths to thousands of seconds in various sources, and span at least three decades in one source, MXB 1730-335 (Lewin et al. 1976). This source also shows a correlation between the integrated energy in a given burst and the length of the following interval. Although an identification is by no means well established, it will be shown that this correlation is to be expected for a particular limiting case of the model considered below. The decay may be another clue to the nature of these sources; however Canizares (1976) has suggested that this may be due to processing of the radiation in a surrounding medium, and may thus mask an entirely different and more rapid decay of the original burst. There is also some indication that these sources are associated with globular clusters (Clark et al. 1976).

Models for compact x-ray sources have generally been based on collapsed objects, i.e. black holes, neutron stars and white dwarfs. This approach is based on the assumption that the sources are for the most part fueled by accretion. Within that assumption the luminosity is determined by the accretion rate and the depth of the gravitational potential well, and the radiation temperature (for thermal emission) is determined by the well depth alone. The classes of collapsed objects cover the range of our understanding of stellar remnants. The electron-degenerate white dwarfs are well understood and are known to exist in non-x-ray binaries. The neutron-degenerate neutron stars are less well understood, but have been detected as pulsars. One is known to be in a non-x-ray binary. Black holes are poorly understood, but seem to be required by accepted treatments of relativity and current understanding of stellar structure and evolution. A massive (> 5 solar masses) variable x-ray source would be a strong candidate for the first detection of a black hole. The present work assumes a white dwarf as the collapsed object. We will examine the expected emission of x-rays from the impact of the accreting matter in both static and dynamic models, and particularly the temporal behavior of the emission.

Studies of accretion effects on white dwarfs have been done by many authors. Mestel (1952) assumed that the energy of the accreting matter went into heating of the degenerate core and concluded that this could result in a supernova explosion. Later authors concluded that most of the energy remains in the non-degenerate layers, eventually producing a hydrogen burning shell which leads to a nova rather than a supernova. In particular, Rose and co-workers, and Starrfield and co-workers have done a great deal of work on the details of the detonation process in what has come to be the canonical model for a nova.

In this picture novae are white dwarfs in binary systems. The collapsed star accretes hydrogen from the companion. A layer of non-degenerate matter builds up on the surface in hydrostatic equilibrium, gradually raising the temperature and density at the bottom of the layer. Eventually the gas reaches the regime of thermonuclear burning and there is a thermonuclear "runaway" due to the strong temperature dependence of the reaction rates. This finally ejects the outer layers of the star to produce the nova outburst.

In the nova models there is an implied assumption that, at the time of detonation, the accretion rate has decreased to the point of being negligible. The question of interaction between the ejected shell and the gas flow is not considered. While matter accretes at rates comparable to those necessary to produce a detonation in the first place, the nova must be an x-ray source. This follows from the fact that the accretion flow will be supersonic with a velocity determined by the gravitational potential of the star. (If the flow is sufficiently dense to be sonic, the entire region around the star will be at x-ray temperatures and opaque.) When the shell encounters the gas flow, the bulk velocity will be thermalized in a shock, and the resultant temperature (which depends only on the velocity) will produce thermal x-rays.

While it is certainly possible for the source to detonate after mass transfer has stopped, it is not a necessary consequence of the model. The time to reach detonation depends on the accreted mass. (The standard models assume relatively cold white dwarfs and neglect the kinetic energy of the accreted matter. Changing either assumption should decrease the evolution time.) Thus for larger accretion rates the time scale is shorter. However, the accretion rate depends primarily on conditions in the companion star, and should not be affected by the evolution of the burning layer, unless the luminosity approaches the Eddington Limit. One thus expects that in at least some cases the detonation will occur while the flow is large, producing an x-ray source.

For simplicity we assume the accretion flow is radial, spherically symmetric and in free-fall. A full analysis of this model would involve extensive numerical work on the details of the evolution of the burning layer. Since the x-ray emission is due to the interaction of the shell and the accretion flow, such a study has not been undertaken. Rather, the basic idea of the nova models is assumed, and the ejected matter is described in terms of parameters which could in principle be determined by such a study.

In order to determine a reasonable range of parameter values, we examine some of the details of the nova models, in particular those of Starrfield et al. (1974a,b; hereinafter S4). It should be remembered that these were attempts to match the observed characteristics of novae, requiring the ejection of masses of the order of 10^{26} g at velocities of several thousand kilometers per second. In order to achieve this, S4 assumes that core mixing has enhanced the CNO abundances in the burning layer by large factors. Without this enhancement the computations produce detonations, but with ejected masses much lower than those desired. Since these models "fail", they are not presented in detail.

The evolution seems to depend rather strongly on the initial white dwarf model assumed. In S4 the "successful" models are based on fairly standard cold white dwarfs. Since the depth of the burning layer (and thus the overlying mass) depends on the temperature structure of the outer layers, the mass will be reduced by assuming a hotter initial star, as well as by considering the heating due to the kinetic energy of the accreting matter. It is interesting to note that much of this energy will be radiated away in a standing shock at the surface during the time preceding the outburst. A nova thus may be preceded by a steady x-ray source.

The surface velocity produced by the detonation is determined by two effects. The first is the emergence of a shock at the surface, generated by the detonation deeper in the layer. While S4 indicates temperatures as high as 4×10^6 K due to the shock, the outward-moving layers cool rapidly by adiabatic expansion. The second effect is the acceleration of the overburden by radiation pressure even before the shock goes by. This effect seems to be important for all but the weakest detonations, and produces velocities which are comparable to those produced by the emergent shock. The temperatures found for this process are lower than the LTE value in the S4 calculations.

Based on the above, we accept the masses of S4 as upper limits to the ejected mass. Since the acceleration mechanisms do not depend as strongly on the burning depth, the velocities probably do not change much, and are chosen as typical values. The temperature at the surface is taken to be less than 10^6 K except in the very earliest stages of the motion, a point which will become important in considering the spectrum of the x-rays produced.

A given outburst is thus characterized by the initial mass, M_o, and velocity, V_o, of the ejected shell. The accretion flow is described by density ρ_a and (free-fall) velocity v_a. The accreting gas is taken to be fully ionized. The value of v_a is determined by the mass and radius of the star. The value of ρ_a is a free parameter subject to constraints discussed in Chapter II. The initial (maximum) shell velocity is taken to be of the order of 10^8 cm s^{-1}, and the value of M_o is less than (possibly much less than) 10^{26} g. The temperature of the surface of the optically thick shell is taken to be several times 10^5 K, but this is discussed further in Chapter VII. For repetitive sources it will also be necessary to consider the relation between the parameters describing successive outbursts.

CHAPTER II

GENERAL CHARACTERISTICS AND CONSTRAINTS

§1. Introduction

The details of a model for an x-ray source are usually developed with the aim of reproducing or predicting the detailed behavior of the source. There are, however, several observational and theoretical constraints on the model - e.g. energy source, energy conversion mechanism, and opacity - which provide some information about the source independent of the details of the model, and which serve to define the allowed regime of physical parameters. The energy source and conversion mechanism in particular have forced nearly all authors in this area to assume the now canonical binary system with accretion of gas onto a compact object. This follows quite simply from the observed fact that the spectra of compact x-ray sources are thermal or power laws. One could perhaps concoct a model based on non-thermal processes which would yield appropriate luminosities for some sources; however, accretion onto a compact object offers a simple mechanism for both the overall energy flow and the observed temperatures for a thermal spectrum. An appropriate conversion process is provided by a shock at the surface of the compact object.

Within this framework of assumptions we can derive some general limits on the accretion density and luminosity, in §3, and in §4 we consider the effects of gross energy balance on a white dwarf in an equilibrium pulsation mode. Both sections assume radial accretion;

although it is known (e.g. Pringle and Rees 1972) that the accretion process produces a disk of gas near the compact object, the assumption of radial inflow simplifies the analysis. Some effects of relaxing this assumption are discussed in Chapter VII. In §4, for the equilibrium analysis, we assume a moving shell. It should be noted that similar work has been done by Cameron (1966) for a normal mode pulsation of the entire star, and by DeGregoria (1974) and DeGregoria and Woltjer (1973) for a model based on radiation pressure modulation of the flow density into a standing shock. The latter found no stable periodic solutions.

§2. Observational Constraints

Having assumed a shock as the energy conversion mechanism, we can reach some immediate conclusions as to the appropriate range of physical parameters for a typical source. In particular, the radiation temperature provides an immediate check on the self-consistency of the model assumptions. For any shock model the maximum temperature behind the shock is given by $T_{max} \simeq 2 \times 10^{-9} v^2(t)$, where v(t) is the shock velocity in the frame of the accreting gas. For a free-fall flow onto a stationary surface (a standing shock) this is just the escape velocity for the source object. If the surface is not stationary, v is the sum of the escape velocity and the instantaneous intrinsic surface velocity. This becomes important in the details of the model; for the present purposes we note that it seems unlikely, particularly so in a periodic source, that the surface velocity is very much larger than the escape velocity. Thus, for a white dwarf (or any other object for which the ratio of mass to radius is known) the radiation temperature determines, at least approximately, the mass of the source. In principle this could be determined exactly, along with the initial shell velocity, by comparing the temperatures in the leading and trailing edges of the pulse. In practice, however, the observations do not generally have sufficient time resolution and sensitivity to permit this analysis. Most compact x-ray sources seem to have radiation temperatures of the order of 10^8 K, which is consistent with the free-fall velocities of white dwarfs.

If the distance - and thus the luminosity - is also known, one can estimate the density of the accreting gas in the shock region for a given scale size. For luminosities of order 10^{36} erg s^{-1}, white dwarf scale sizes imply a mass density of the order of 10^{-8} g cm^{-3}. This is also subject to an opacity limit derived below.

Finally, if an independent determination of the mass can be made (e.g. in optically observed binaries), the temperature-velocity relationship can be used to fix the radius observationally (again subject to the assumption of free-fall). In this case all of the major parameters are fixed, and the entire class of models can be rigorously tested for consistency with regard to a particular object.

§3. Opacity Limits

As has been noted by several authors (e.g. Fabian, Pringle and Rees (1976)), the assumption that the radiated energy is supplied by accretion, kinetic energy implies an upper limit to the luminosity of such a source. Conservation of mass requires that the mass accretion rate be given by

$$\frac{dM}{dt} = 4\pi R^2 \rho(R) v(R) \tag{2.1}$$

where R is the surface radius. The energy available per unit mass is just

$$E_K = \frac{GM_*}{R}$$

where M_* is the stellar mass and G is the gravitational constant. The minimum accretion rate for a given luminosity, L, is then

$$\frac{dM}{dt} = \frac{L}{E_K} \tag{2.2}$$

and

$$\frac{LR}{GM_*} = 4\pi R^2 \rho(R) v(R) \; . \tag{2.3}$$

Now for free-falling matter, $v(R) = (2\ GM_*/R)^{1/2}$ and the necessary value of the surface density is given by

$$\rho(R) = \frac{L}{\sqrt{2}} \left(\frac{R}{GM_*}\right)^{3/2} \frac{1}{4\pi R^2} \; . \tag{2.4}$$

In terms of $\Gamma_{26} \equiv 10^{-26}\ GM_*$ and $R_8 \equiv 10^{-8} R$, this gives

$$\rho(R) \simeq 5.6 \times 10^{-45} R_8^{-1/2} \Gamma_{26}^{-3/2} L \; . \tag{2.5}$$

The other limit on $\rho(R)$ is derived from the requirement that the x-rays be able to escape, i.e. the accreting gas must be optically thin. Assuming complete ionization, the dominant source of opacity for the energy range of interest is simple Thomson scattering. The optical depth is then given by

$$\tau = \int_R^X \frac{\rho(r)}{m_p} \sigma_T \, dr \tag{2.6}$$

where X is the distance to the outer edge of the accreting gas.

Since we are assuming free-fall (radial) inflow, $\rho(r) = \frac{R^2}{r^2} \rho(R)$ and

$$\tau = \frac{\sigma_T}{m_p} R^2 \rho(R) \int_R^X \frac{1}{r^2} \, dr = \frac{\sigma_T}{m_p} R^2 \rho(R) (\frac{1}{R} - \frac{1}{X}) \ . \tag{2.7}$$

If we take $X \simeq 10 \ R$ this implies that

$$\rho(R) \lesssim 3 \times 10^{-8} R_8^{-1} \tag{2.8}$$

to avoid quenching of the x-rays. Combining this with Equation (2.5) we then find

$$L \lesssim 5.3 \times 10^{36} R_8^{-1/2} \Gamma_{26}^{3/2} \text{ erg s}^{-1} \ . \tag{2.9}$$

For white dwarfs we thus expect luminosities no larger than a few times 10^{36} erg s^{-1}.

§4. Equilibrium and Stability Considerations

One type of source behavior to which white dwarf models might be applied is, as mentioned in Chapter I, the pulsating x-ray sources. This may be taken to include the transient pulsating sources, as well as Her X-1 and Cen X-3. The existence of a well defined pulsation period clearly requires a model which can exist in some equilibrium oscillatory state. In earlier white dwarf models (e.g. Cameron 1966, 1974), it has frequently been assumed that the oscillation is a normal mode vibration of the entire star, fueled by nuclear burning. Katz and Salpeter (1974) have argued that the accreting hydrogen will burn as fast as it arrives, and that the pulsations will damp out as an extended hydrogen burning shell develops.

Guthrie and Tademaru (1975), however, argue that this assumption of rapid burning on the surface is not valid for a pulsating source, although it may be accurate in the case of a steady source. This point reflects a somewhat subtle but quite important distinction between this and other considerations of white dwarf models.

One of the main conclusions of the nova work mentioned previously is that nuclear burning in the atmosphere of the accreting star is triggered well below the surface. For very low accretion rates, the burning may be slow enough for the outer layers to expand as they are heated, eventually perhaps producing a steady source which burns the hydrogen on the surface. However, for accretion rates well below those indicated for compact x-ray sources, the nova computations produce a rapid thermonuclear source which blows off the overlying material. Whether or not this shell reaches escape velocity is not germane to the point at issue; once a shell has been blown off, the burning layer expands, cools and quenches itself. Thus, once the burning layer has been triggered, the hydrogen will burn only intermittently - if the shell escapes, at long intervals; if the shell does not escape, at those times when the returning shell compresses and heats it.

During outward motion of the shell, a shock is established in the accretion flow. In passing through this shock, the kinetic energy of the infalling material is thermalized and rapidly - indeed "instantaneously" on the time scale of the shell motion - lost via radiation. During this phase of the motion, energy is lost from the system, both from the accretion flow and from the shell, which is also doing work on the gas. This energy can be returned to the shell only during the infall phase, when the unthermalized accretion flow does net work on the shell. The shell kinetic energy as it returns to the surface determines the degree of compression of the burning layer, and thus the impulse imparted to the shell for the next cycle.

If the energy acquired during the infall and compression phases is greater than or less than the energy imparted by the previous impulse, the conditions in the burning layer will adjust to the net gain or loss of energy so as to increase or decrease the burning rate, respectively. This argument was put forth by Cameron (1966) to explain the stability of normal-mode-type models, but it is also applicable here. It implies that, for a relatively constant burning depth and accretion flow, there exists a stable equilibrium value of the shell ejection velocity which is determined by energy equilibrium during one cycle. This stability is with respect to changes in the burning rate; the response of the system to changes in other parameters will be considered later in this work. The important point is that the burning rate is determined not by the rate of accretion of matter alone, but by the rate of accretion of kinetic energy from the infalling gas. The burning layer becomes, in effect, a spring.

Examples of equilibrium calculations. As examples of the application of this equilibrium criterion, we consider two cases in which the shell motion is described by simple analytic functions of time. In the detailed models this will not generally be the case.

The system loses energy only during outward motion, defined as positive shell velocity, $v_s(t) \geq 0$. For a spherical shell, the total work done on the gas flow by the surface is

$$W_L = 4\pi R^2 \rho \int_0^T [v_a + v_s(t)]^3 \, dt \qquad (2.10)$$

where R is the (~ constant) shell radius, ρ is the density of the accreting gas, v_T is the (free-fall) accretion velocity, P is the period of the shell motion, and T is the turn-around time for the shell, $0 \leq t \leq T < P$. Note that this expression approaches a non-zero limit as $v_s(t)$ goes to zero. This amounts to considering only the strong-shock limit; the thermalization efficiency within the shock region drops rapidly as the shock becomes weak.

Since momentum must be conserved, the work done by the gas flow during one period is

$$W_G = 4\pi R^2 \rho v_a^3 P \ . \qquad (2.11)$$

The equilibrium state is determined by setting $W_G = W_L$, which yields

$$v_a^3 P = \int_0^T [v_a + v_s(t)]^3 dt \ . \qquad (2.12)$$

Expressing $v_s(t)$ as $v_s(t) = V_o f(t)$ this becomes

$$\gamma^3 P = \int_0^T [\gamma + f(t)]^3 dt \ , \qquad (2.13)$$

where $\gamma \equiv v_a/V_o$. To be physically meaningful, $f(t)$ must be zero at $t = 0$ and $t = T$ and must have a single maximum on that interval. Evaluation of the integral then reduces the problem to the solution of a cubic equation in γ.

For example, suppose that the time dependence were given by $f(t) = \sin(2\pi P^{-1} t)$ on $0 \le t \le P/2$. The integral is then

$$I = \int_0^{P/2} [\gamma + \sin(\frac{2\pi}{P} t)]^3 dt \qquad (2.14)$$

which may be evaluated to give

$$I = \frac{P}{2} [\frac{\pi}{2} \gamma^3 + 3\gamma^2 + \frac{3\pi}{4} \gamma + \frac{2}{3}] \ , \qquad (2.15)$$

and Equation (2.13) becomes

$$\frac{3\pi}{2} \gamma^3 - 3\gamma^2 - \frac{3\pi}{4} \gamma - \frac{2}{3} = 0 \ . \qquad (2.16)$$

This equation has only one real positive root, at $\gamma = 1.17$, implying that for equilibrium in the energy flow $V_o = V_{critical} \simeq .86\ v_a$.

As another example, let f(t) be a symmetric, linear function of time

$$f(t) = 4t/p \quad ; \quad 0 \leq t \leq P/4$$

$$= 2(1 - 2t/P) \quad ; \quad P/4 \leq t \leq P/2 . \tag{2.17}$$

The cubic in this case is

$$\gamma^3 - \frac{3}{2}\gamma^2 - \gamma - \frac{1}{4} = 0 \tag{2.18}$$

for a critical velocity $V_c \simeq .51\ v_a$. Note that, although the critical velocity is of the same order as the accretion velocity (as one would expect), the exact value of V_c depends on the form of f(t). In general, the smaller the integral of v_s over time, the larger is the necessary critical velocity, since the loss rate is velocity dependent, as well as the total energy loss.

Although in the cases of some of the more interesting periodic pulsation models it will not be possible to write down a simple explicit form for f(t), the energy balance principle illustrated here can still be applied. For more realistic equilibrium calculations, one must also realize that the radiation losses do not necessarily stop at the moment of turnaround ($v_s(t) = 0$). If the accretion flow is highly supersonic there will still be a shock even for downward (negative) velocities of the shell. This should, however, be a rather small correction. The loss rate goes as the cube of the relative velocity, so that as $v_s \to - v_a$, $W_L \to 0$ quite quickly.

CHAPTER III

RADIATION ANALYSIS

We are interested here in time variable x-ray sources. In order to model such a source one must specify the relevant radiation mechanisms and the physical conditions in the source as functions of both space and time. For problems involving shocks this requires the solution of the full set of gasdynamic equations. In general, exact analytical solutions of these equations are quite difficult, and such problems are usually solved by extensive numerical analysis.

For the models considered herein, however, it is possible to reduce the numerical complexity considerably. As mentioned in Chapter I, the approximate time scales for variability in compact x-ray sources are of the order of seconds or longer (with the notable exception of the most rapid burst sources). The radiative time scales, however, may be much shorter. For the temperatures of interest (10^7 - 10^8K), and the densities indicated in Chapter II, the free-free cooling times are of the order of tenths of seconds, or even shorter. If the overall time scale is characteristic of the motion of the shock, then the cooling time is short compared to the dynamic time scale. Under these conditions the shock velocity changes by very little during a cooling time.

We limit our investigation to the regime in which the shock is radiative, the shock motion being uncoupled from the conditions in the cooling region. We consider then a series of constant velocity (or standing) shocks, the velocity being determined by processes unrelated to the radiative losses. This reduces the gasdynamics problem to that of determining the equilibrium flow in one spatial dimension for a transparent radiating gas. The process governing the velocity of the shock as a function of time will be considered in Chapters IV and V.

The physical conditions behind a standing shock at the surface of a white dwarf have been investigated by a number of authors, especially Aizu (1973) and Fabian, Pringle and Rees (1976). Aizu develops an analytic approximation to the run of parameters in the cooling region. Both Aizu and Fabian et al. find that for many purposes it is sufficient to consider the cooling region as being homogeneous in temperature and density out to a sharp cutoff. For the purposes of this investigation a more detailed analysis is desired, for which numerical solution of the flow equations are developed.

The relevant equations are the conservation equations of mass, momentum and energy for a stationary-state flow in one dimension. Thus, the gas flows through the cooling region so that the conditions at each point depend only on the distance from that point to the shock. Mathematically, this means that $\partial/\partial t = 0$ and all time derivatives can be expressed as $d/dt = v d/dz$. Assuming the perfect gas law, the equations are then

$$u \frac{d\rho}{dz} = - \rho \frac{du}{dz} \tag{3.1}$$

$$\rho u \frac{du}{dz} = \frac{k}{m} \left(T \frac{d\rho}{dz} + \rho \frac{dT}{dz}\right) \tag{3.2}$$

$$\rho u \left(\frac{3}{2} \frac{k}{m} \frac{dT}{dz}\right) = - \frac{k}{m} \rho T \frac{du}{dz} - \varepsilon_{ff} \tag{3.3}$$

where ρ, u, T are density, velocity and temperature, respectively. Here ε_{ff} is the radiative loss rate per unit volume and may be expressed as

$$\varepsilon_{ff} = .5 \times 10^{21}\, \bar{g} \rho^2 T^{1/2} \text{ erg cm}^{-3} \text{ s}^{-1} \qquad (3.4)$$

where $\bar{g}$ is the Gaunt factor. For the cooling rate calculations $\bar{g}$ may be taken as 1.0; however in computing the spectrum the energy dependence is retained. By using as the initial conditions the jump conditions for a strong adiabatic shock with specified velocity and density, we reduce the flow problem to an initial value problem in one dimension. This can be easily solved via numerical methods.

The computations are carried out using a fourth order Runge-Kutta scheme, but the coupled derivatives complicate this somewhat. By substituting (3.1) into (3.2) and the resulting expression for du/dz in (3.3), one obtains an equation for dT/dz involving only the variables ρ, u and T, the derivatives being eliminated. This is used to evaluate dT/dz at each net point. For each space step the T derivative is extrapolated, the other derivatives evaluated, and all are then corrected to the center of the interval using a standard forward and backward finite differencing technique (see e.g. Richtmyer 1957). These new values of the derivatives are then used in the Runge-Kutta routines. For an Eulerian initial value problem such as this, the problem of instabilities may be simply avoided by using a variable step size as the derivatives become large.

In comparing the runs of this model with the standing shock calculations it should be remembered that the shock is, in fact, not at the stellar surface. Because of this a different criterion for ending the calculation is used. The solutions of Aizu show the variables changing rapidly (steep derivatives) right down to the stellar surface where an infinite sink boundary condition is applied. Although it is not apparent on this scale, the models shown in Figure 3-1 level off. This is due to the fact that a temperature cutoff has been used, rather than one based on position. In particular, the density levels off as expected for a radiative shock with $\rho_{final} = \rho_{initial} (v_i/v_f)$ and the initial values are those immediately behind the shock. The scale is chosen to show the curvature in the density function. The minimum temperature is determined by the history of the underlying mass shell, and has been arbitrarily set at various levels between 10^5 and 10^6 K. In Figure 3-1 the cutoff is at 5×10^5 K. Although the temperature chosen does not greatly affect the depth of the cooling region, it may strongly affect the spectrum of the escaping radiation. This is due to the effects of inverse Compton cooling if the cutoff is too high (Katz and Salpeter 1975). For reasons outlined in Chapter IV and in Guthrie and Tademaru (1975) the cutoff temperature should be less than 10^6 K.

The distance D_{ff} in Figure 3-1 is determined by following the analysis in Fabian, Pringle and Rees (1976). They assumed free-falling gas, spherical symmetry, total radiation of accretion energy, and homogeneous cooling layer to obtain a cooling depth, D_{ff}. Their value was expressed in terms of the stellar mass, radius, and accretion rate. A similar expression in terms of velocity and density may be obtained as follows.

We set the luminosity, L, equal to the energy accretion rate;

$$L = M \frac{GM_*}{R_*} \; . \qquad (3.5)$$

For a homogeneous layer this is also given by

$$L = 4\pi R^2 D_{ff} \varepsilon_{ff} \; . \qquad (3.6)$$

For free-falling gas and spherical symmetry

$$M = 4\pi R_*^2 \rho v \qquad (3.7)$$

and

$$v = \left(\frac{2GM_*}{R_*}\right)^{1/2} \; . \qquad (3.8)$$

We may thus write

$$\frac{1}{2} \rho v^3 = D_{ff} \varepsilon_{ff} \qquad (3.9)$$

In terms of ρ and v, ε_{ff} is given by

$$\varepsilon_{ff} = 3.76 \times 10^{17} \rho^2 v \qquad (3.10)$$

where the strong adiabatic shock values are assumed throughout the layer. Writing $v = v_8 \times 10^8$ cm s^{-1} and $\rho = \rho_{-8} \times 10^{-8}$ g cm^{-3} one has

$$D_{ff} = 1.33 \times 10^6 \frac{v_8^2}{\rho_{-8}} \; . \qquad (3.11)$$

In Figure 3-1 we see that this is in reasonably good agreement with the computations.

Figure 3-1a: Run of temperature, bulk velocity and density relative to initial values in cooling layer of radiative shock at shock velocity $v_s = 3 \times 10^8$ cm s^{-1}, $\rho_a = 10^{-8}$ g cm^{-3}.

Figure 3-1b: Run of temperature, bulk velocity and density relative to initial values in cooling layer of radiative shock at shock velocity $v_s = 6 \times 10^8$ cm s^{-1}, $\rho_a = 10^{-8}$ g cm^{-3}.

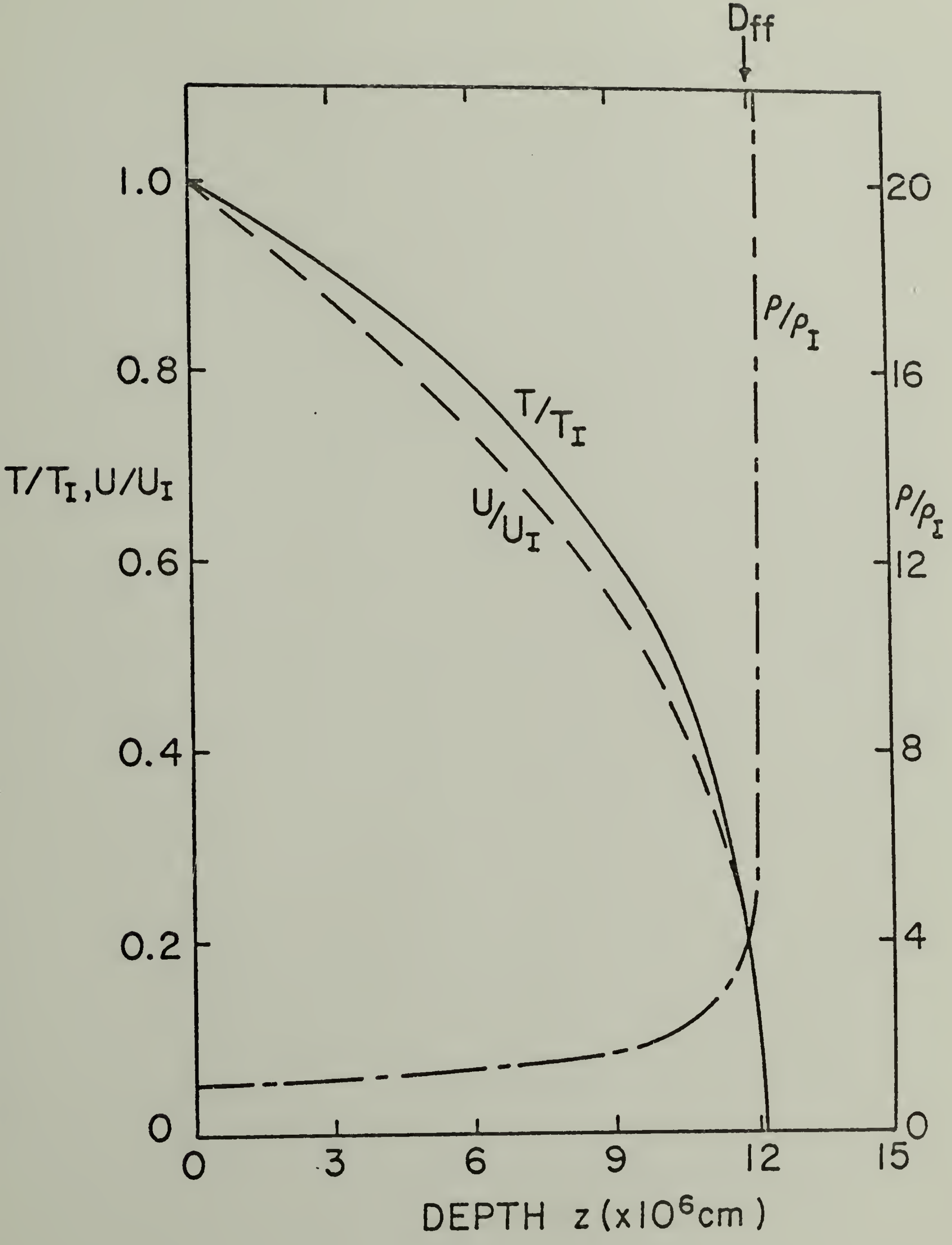

D_{ff}
1.0
0.8
0.6
0.4
0.2
0
$T/T_I, U/U_I$
T/T_I
U/U_I
ρ/ρ_I
ρ/ρ_I
20
16
12
8
4
0
0
3
6
9
12
15
DEPTH z ($\times 10^6$ cm)

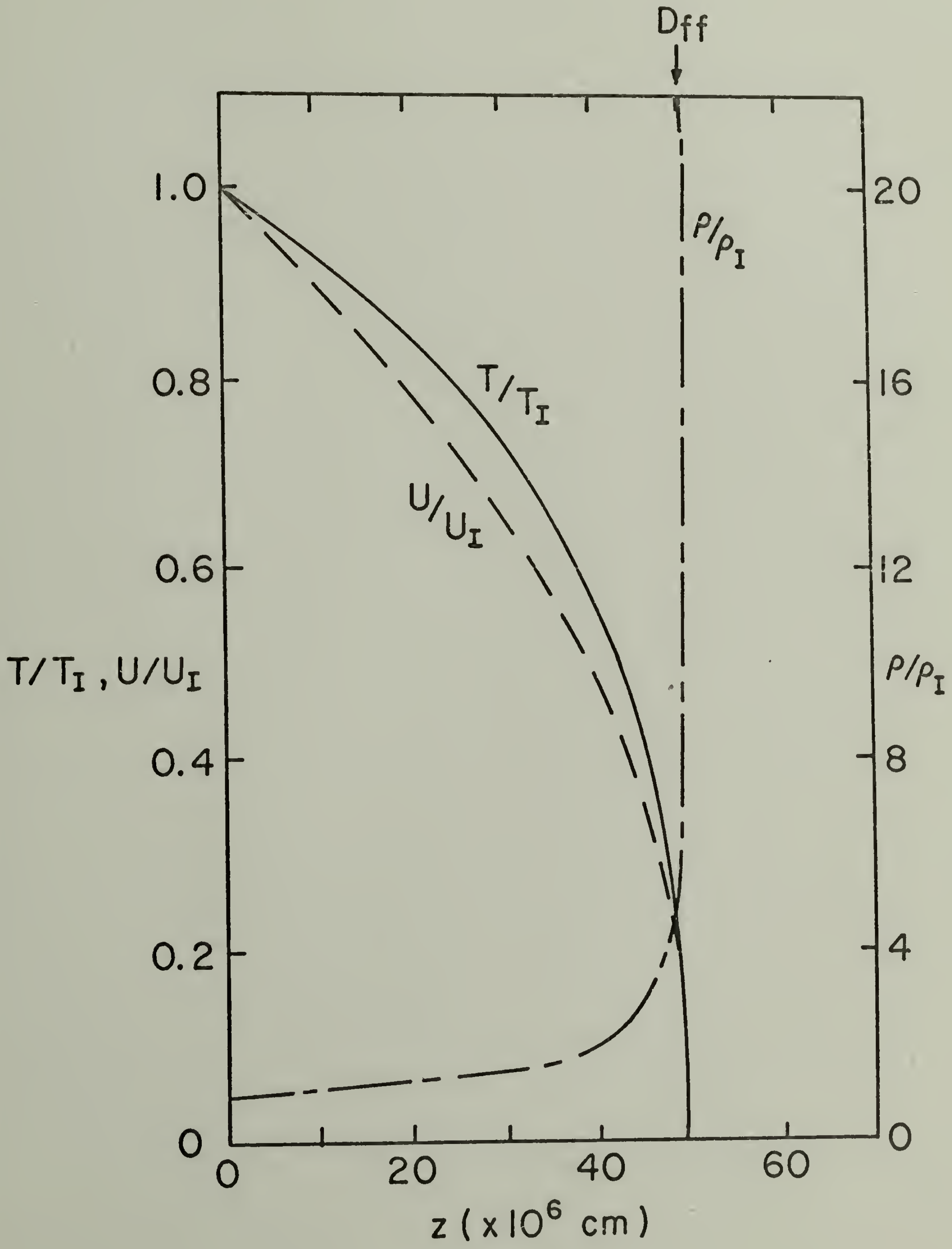
Dff
1.0
0.8
0.6
0.4
0.2
0
T/T_I, U/U_I
20
16
12
8
4
0
ρ/ρ_I
ρ/ρ_I
T/T_I
U/U_I
0
20
40
60
z (x 10^6 cm)

Knowing the physical conditions at each point we can now calculate the radiation emitted from the cooling region. For the total luminosity, L_T, we use simply the integrated emissivity (Equation 3.4) at depth z in a layer of thickness dz and sum over z. This gives a luminosity per unit area which is multiplied by the surface area of the shell to obtain L_T.

We also wish to obtain the spectrum of the radiation. The expression for the spectral emissivity is (Blumenthal and Tucker 1974)

$$S(E) = 1.6 \times 10^{-20} \frac{n^2}{T^{1/2}} \left(\frac{E}{kT}\right)^{-0.4} e^{-E/kT} \text{ erg cm}^{-3} \text{ s}^{-1} \text{ Kev}^{-1} \qquad (3.13)$$

where n is the number density in cm^{-3} and E is in Kev. The energy dependence of the Gaunt factor has been retained in an approximation appropriate for E comparable to kT. Again we sum over z to obtain the spectrum shown in Figure 3-2. A spectrum for a homogeneous region at $T = 10^8$ K is shown for comparison. In both of these spectrum and luminosity examples we have assumed that the cooling region is optically thin, and that there is negligible inverse Compton cooling.

In comparing such a spectrum with observations we must remember that this curve is the instantaneous spectrum; observational spectra will always be integrated over some time interval. In Chapter VI the time development of the spectrum during an outburst is computed in a way which makes comparison with observations somewhat more straightforward.

Figure 3-2: Computed spectrum (see text) and spectrum of homogeneous region at $T = 10^8$ K.

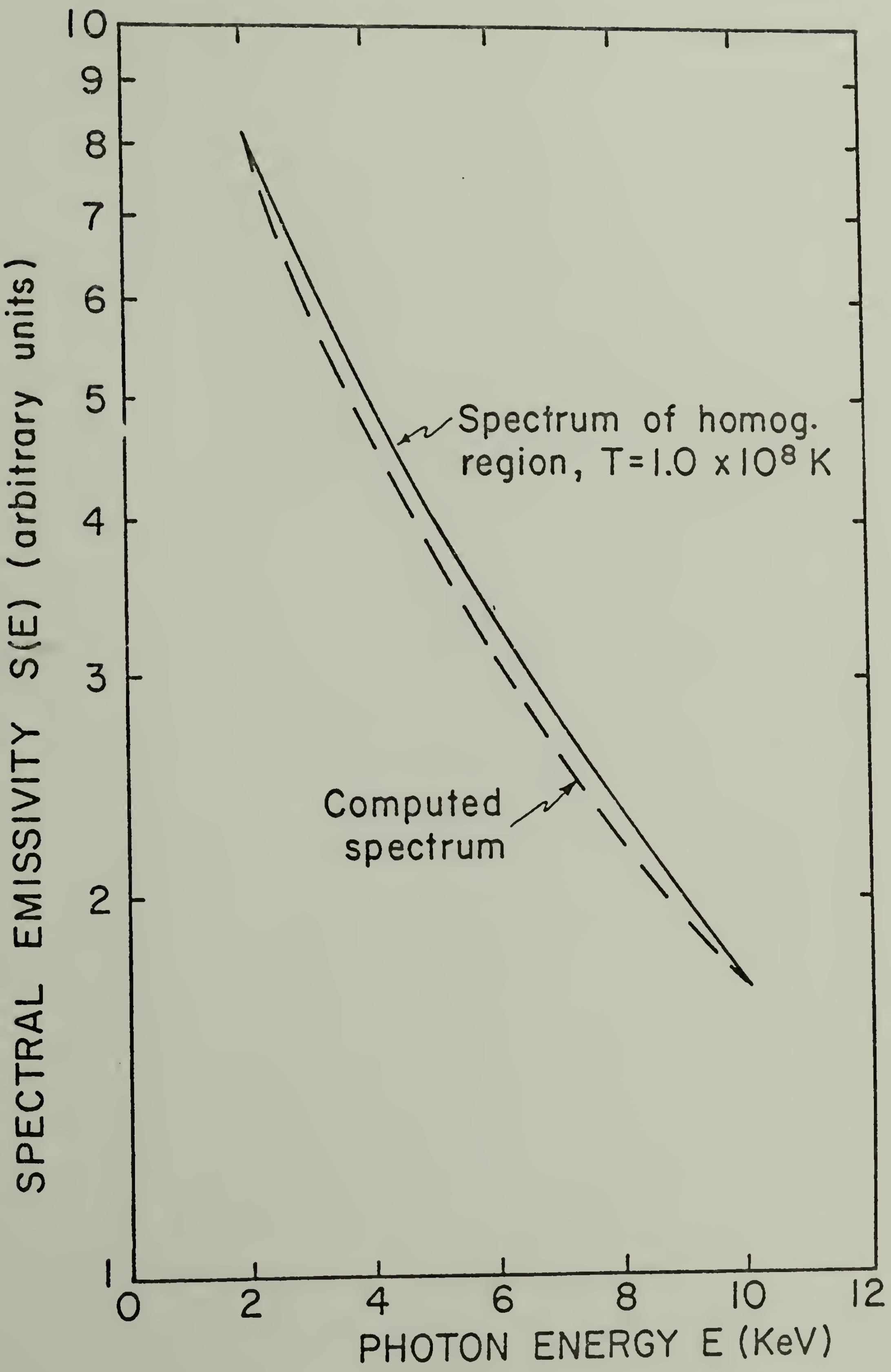
SPECTRAL EMISSIVITY S(E) (arbitrary units)
10
9
8
7
6
5
4
3
2
1
0
2
4
6
8
10
12
PHOTON ENERGY E (KeV)
Spectrum of homog. region, $T=1.0 \times 10^8$ K
Computed spectrum

CHAPTER IV

VELOCITY OF THE SHOCK

The next step in the analysis of the model is to determine the velocity of the shock as a function of time. This is divided into two parts; an acceleration phase and a decay phase. Because the acceleration phase is controlled by the details of the nuclear burning, we are unfortunately limited to a rather qualitative analysis based on the nova calculations mentioned above. The decay phase, however, can be treated fairly rigorously.

§1. Acceleration

In considering the ejection of nova shells, S4 find two processes to be of importance in determining the ejection velocities. There is, in general, a shock generated by the burning layer which then propagates to the surface. For some models, however, they also find that radiation pressure produces significant surface velocities, reducing the relative shock intensity and thus producing lower surface temperatures for the same surface velocity. Although the relative importance of these two effects cannot be determined for a given model without a detailed treatment of the burning layer, it is possible to estimate the pulse rise time scales for both.

a) Radiation pressure case. In the case where radiation pressure dominates, S4 find that, particularly in the later stages of the ejection process, the radiation pressure force can exceed gravity by a factor of as much as 5 to 10. Defining X as the ratio of the radiation force to gravity (and assuming that χ is approximately constant during the time scales of interest) one may write

$$v \simeq (\chi - 1) gt$$

where g is the surface gravity. For white dwarf gravities and final velocities of the order of several times 10^8 cm s^{-1}, this indicates rise times of several tenths of seconds. Such rise times are indeed observed in both pulsating (Doxsey et al. 1973) and bursting (Clark et al. 1976) x-ray sources.

b) Emergent shock case. The case of an emergent shock is somewhat more complicated. Consider a density distribution

$$\rho = bx^{\delta}$$

where x is measured inward from the surface of the star. The problem of shock propagation outward (i.e. $\dot{x} \leq 0$) in such a distribution has been considered by Zel'dovich and Raizer (1966) and references therein. They find solutions of the form

$$x_s = At^{\alpha}, \quad \dot{x}_s = \alpha A t^{\alpha-1} ,$$

where t is defined as minus the usual time variable and t = 0 at x = 0. The shock analysis yields α as a function of δ.

Now consider the observable luminosity due to this shock as it approaches the surface. The luminosity per unit area due to free-free emission is

$$L_s = C_{ff}\rho^2 T^{1/2}$$

where C_{ff} is a constant, ρ and T are the density and temperature behind the shock. Since the shock is initially adiabatic, this becomes

$$L_s = C_{ff}C_s b^2 x_s^{2\delta} \dot{x}_s$$

where C_s includes all the constants in the post-shock dependence of ρ, T. In terms of t, this becomes

$$L_s = C_{ff}C_s b^2 \alpha A^{2\delta+1} t^{\alpha(2\delta+1)-1} .$$

Note that as $t \to 0$, the temperature increases but the luminosity decreases, due to the density dependence. This approximation should be valid until the overlying material becomes transparent and the shock motion becomes radiation dominated.

We wish to determine the observable luminosity as a function of time as the shock approaches transition. We approximate this by assuming that the shock is adiabatic for overlying optical depth $z \geq 1$ and radiative thereafter. The adiabatic phase must then be corrected for opacity to get the observed luminosity.

The observed luminosity, L_{ob}, is related to the shock luminosity by

$$L_{ob} = L_s e^{-\tau}$$

where

$$\tau = K\int_0^{x_s} \rho(x)dx$$

and K is the absorption coefficient. Thus

$$\tau = \frac{Kb}{\delta+1} x^{\delta+1} = \frac{Kb}{\delta+1} A^{\delta+1} t^{\alpha(\delta+1)} .$$

We then have for L_{ob}

$$L_{ob} = C_{ff} C_s b^2 \alpha A^{2\delta+1} t^{\alpha(2\delta+1)-1} \exp\left(- \frac{Kb}{\delta+1} A^{\delta+1} t^{\alpha(\delta+1)}\right) .$$

Note that for large values of t the exponential dominates, i.e. the shock is not seen, as expected. The observed luminosity will then increase, even though the shock luminosity decreases. The time scale for this rise is determined by the values of K, b, A and δ.

In order to consider a numerical example we must find some approximation to the density structure. We can estimate the amount of mass involved by noting that the total kinetic energy of the shell must be comparable to the integrated energy loss over one pulse. For many x-ray sources, subject to the constraints of this model, a reasonable number for this is $E \lesssim 10^{38}$ erg. We then write

$$4\pi R_o^2 M_o V_o^2 \simeq 10^{38} \text{ erg}$$

where R_o is the stellar radius, M_o is the mass per unit shell area, and V_o is the maximum velocity of the shell. Since V_o and R_o are fixed, at least to order of magnitude, by the model assumptions, we obtain $M_o \sim$ 10's to 100's of g-cm^{-2}. If the shell depth is taken to be on the order of 10^6 cm (S4), we then have a mean shell density $\bar{\rho}_s \simeq 10^{-4}$ g-cm^{-3}. In finding reasonable values of the parameters b and δ we assume that the outer layers have expanded from their equilibrium configuration in such a way as to change the power law, but maintain the constant of proportionality. For white dwarf structures this gives $b \sim 10^{-12}$ in CGS units. Then the expression for $\rho(x)$ gives a value for δ of 4/3 when applied to the outer shell. The corresponding value for α is approximately 0.76, and assuming the opacity is primarily due to electron scattering gives $K \simeq 0.4$.

In order to approximate A, we assume that the peak luminosity occurs at $\tau = 1$. We define t' such that $\tau(t') = 1$, i.e.

$$t' = \left(\frac{\delta+1}{KbA^{\delta+1}}\right)^{1/\alpha(\delta+1)} .$$

We then match the adiabatic and radiative solutions at t'. For typical conditions this implies a peak velocity of the order of 10^8 cm s^{-1}. Then $\dot{x}_s(t') = \alpha A t'^{(\alpha-1)} = V_8 \times 10^8$. Substituting for t',

$$\dot{x}_s(t') = \alpha A\left(\frac{\delta+1}{KbA^{\delta+1}}\right)^{\frac{\alpha-1}{(\delta+1)\alpha}}$$

$$\dot{x}_s(t') = \alpha\left(\frac{\delta+1}{Kb}\right)^{\frac{\alpha-1}{(\delta+1)\alpha}} A^{1/\alpha}$$

or

$$A = \left(\frac{\dot{x}_s(t')}{\alpha}\right)^{\alpha} \left(\frac{Kb}{\delta+1}\right)^{\frac{\alpha-1}{\delta+1}} .$$

The exponential term then becomes

$$\exp\left(-\frac{Kb}{\delta+1} A^{\delta+1} t^{\alpha(\delta+1)}\right) = \exp\left(-\left(\frac{Kb}{\delta+1}\right)^{\alpha}\left(\frac{\dot{x}_s(t')}{\alpha}\right)^{\alpha(\delta+1)} t^{\alpha(\delta+1)}\right) .$$

Plugging in the numbers, this gives

$$L_{ob} \propto t^{\alpha(2\delta+1)-1} \exp(-3V_8 \times 10^{4.4} t^{1.8}) \ .$$

We thus expect the luminosity due to the emergent shock to rise on a time scale of ~ 10^{-3} seconds which is essentially instantaneous compared to the currently available x-ray observations.

Although some burst sources show unresolved rises (Lewin et al. 1976), in displaying the model calculations we will assume the radiation pressure case. Since we cannot calculate the details of this case, the "pulses" will be computed for an arbitrarily assumed constant acceleration with a time constant of ~ .5 seconds.

§2. Decay

Once the velocity of the ejected material has reached maximum and starts to decrease, the source luminosity will also begin to decay. In considering this phase of the motion we assume that the ejected material forms a thin, plane-parallel shell.

In principle one might expect the pressure of the gas behind the shell to dominate the equation of motion, at least initially. However, the acceleration process produces a velocity gradient from the position of the initial stellar surface to the surface of the ejected material (S4). This in turn leads to a pressure gradient once the acceleration is complete, producing expansion of some of the gas back toward the star. By the time the layer has relaxed to equilibrium the surface has moved far enough, and the mean temperature and pressure in the layer have been reduced enough, that the motion should be reasonably well approximated by a simple detached shell treatment.

Consider such a shell of mass M per unit area moving upward with velocity v(t). The layer encounters and sweeps up infalling gas of density ρ and downward velocity v_a. In the general case the layer is in a gravitational potential $\phi_G = \Gamma/R$, where $\Gamma \equiv M_* G$, M_* is the stellar mass, G is the gravitational constant, and R is the radial coordinate of the shell, assumed constant. This latter assumption is valid so long as the amplitude of the shell motion is small compared to the stellar radius, which condition is satisfied for all cases considered herein.

Assuming the bulk kinetic energy of the infalling gas is instantaneously lost via radiation at the shock, the equation of motion is determined by the momentum equation. The identical case was considered in Blumenthal et al. (1971) for $v_a = 0$, the classical "snowplow" approximation.

The equation of motion of a unit area of the shell is then

$$\frac{d}{dt}(Mv) = -\rho(v_a + v)^2 - M\frac{\Gamma}{R^2} \tag{4.1}$$

during outward motion

and

$$\frac{d}{dt}(Mv) = \rho(v_a - v)^2 + M\frac{\Gamma}{R^2} \tag{4.2}$$

during inward motion.

The first term on the right in each equation is just the ram pressure of the infalling gas on the shell. Note that v represents the magnitude of $\vec{v}(t)$.

The equation of motion is most easily handled via a Lagrangian approach with the mass per unit area, M(t), as the Lagrangian variable. Thus,

$$M(t) = M_o(t = 0) + \int_o^t dM/dt'dt' \qquad (4.3)$$

and the velocity is related by

$$\dot{M} = \rho(v_a \pm v(t)) \qquad (4.4)$$

where the upper and lower signs refer to outward and inward motion, respectively.

In this formulation the equations become

$$\frac{d}{dt}\,[M(\frac{\dot{M}}{\rho} - v_a)] = -\,\frac{\dot{M}^2}{\rho} - \frac{M\Gamma}{R^2} \qquad (4.5)$$

with

$$v = \frac{\dot{M}}{\rho} - v_a \qquad \text{(outward;}$$

and

$$\frac{d}{dt}\,[M(v_a - \frac{\dot{M}}{\rho})] = \frac{\dot{M}^2}{\rho} + \frac{M\Gamma}{R^2} \qquad (4.6)$$

with

$$v = v_a - \frac{\dot{M}}{\rho} \qquad \text{(inward)}\;.$$

We introduce a new variable, $\mu \equiv M/\rho v_a$, and get the equation

$$\mu\ddot{\mu} + 2\mu^2 - \mu + \frac{1}{v_a}\frac{\Gamma}{R^2}\mu = 0 \qquad (4.7)$$

for both phases of the motion. This equation is now to be solved as a boundary value problem.

This general equation is somewhat intractable, although susceptible to numerical techniques. In order to gain some physical insight, we distinguish two cases which can be handled analytically in their asymptotic limits. The first, called the "quasi-snowplow" (QSP) approximation, is an extension of the classical snowplow to the case $v_a \neq 0$, and considers the motion to be dominated by the momentum flux of the accreting matter. This also corresponds to the limit of low shell mass and large momentum density in the flow, when gravitational effects may be neglected. The second case, which is gravity dominated, is just the usual ballistic problem with a vertical trajectory. This corresponds to the high mass case, where the mass accreted during one period is small compared to the initial shell mass.

a) The QSP limit. In this case we neglect the gravity term. Equation (4.7) then becomes

$$\mu\ddot{\mu} + 2\dot{\mu}^2 - \dot{\mu} = 0 \ . \qquad (4.8)$$

Using standard techniques, we let $P = \dot{\mu}$ and obtain the equation

$$P(\mu \frac{dP}{d\mu} + 2P - 1) = 0 \ . \qquad (4.9)$$

Ignoring the trivial and unphysical solution $P = 0$, $\mu = \text{constant}$,[1] this is separable and integrable, yielding the first integral

$$\dot{\mu} = \frac{1}{2}\,(C_1/\mu^2 + 1) \tag{4.10}$$

where c_1 is the constant of integration.

Equation (4.10) may also be separated to yield

$$\int \frac{d\mu}{C_1/\mu^2+1} = \frac{1}{2}\,t + C_2 \ . \tag{4.11}$$

This integral may be evaluated, and gives

$$\mu - \sqrt{C_1}\,\tan^{-1}\!\left(\frac{\mu}{\sqrt{C_1}}\right) = \frac{1}{2}\,t + C_2 \ . \tag{4.12}$$

For uniqueness we must consider the ambiguity in the inverse tangent function. In general we can write Equation (4.12) as

$$\mu - \sqrt{C_1}\,\mathrm{A\,tan}\left(\frac{\mu}{\sqrt{C_1}}\right) = \frac{1}{2}\,t + C_2 + n\pi\,\sqrt{C_1}$$

where n is an integer. Since C_2 is completely arbitrary at this point we redefine it such that $C_2 \rightarrow C_2 - n\pi\,\sqrt{C_1}$ no matter what n is. Thus in the equations below the inverse tangent takes its principal value and the arbitrary constant of integration is used to remove the ambiguity. The constants remain to be determined from the boundary conditions.

---

[1] $P = 0$, $\mu = \text{const.}$ corresponds to the gravitational limit.

At $t = 0$ we have[2]

$$\mu = \mu_o \equiv \frac{M_o}{\rho v_a}$$

and (4.13)

$$\dot{\mu} = \frac{V_o + v_a}{v_a}$$

where V_o is the initial velocity amplitude of the shell. From Equation (4.10) we then find

$$C_1 = \mu_o^2[2 \frac{V_o + v_a}{v_a} - 1] \equiv \alpha^2\mu_o^2 . \qquad (4.14)$$

We define a "turnaround time," T, such that $v(T) = 0$. Then, for $t = T$, $\dot{\mu}(T) = 1$. We thus require the $\mu^2(T) = C_1$, again from Equation (4.10). This gives

$$\sqrt{C_1}\,(1 - \pi/4) = \frac{1}{2} T + C_2$$

or (4.15)

$$T = 2[\sqrt{C_1}\,(1 - \pi/4) - C_2] .$$

To find C_2 consider $\mu(t = 0)$,

$$\mu_o - \sqrt{C_1} \tan^{-1} \frac{\mu_o}{\sqrt{C_1}} = C_2 \qquad (4.16)$$

---

[2] Throughout this chapter $t = 0$ corresponds to the time of maximum upward velocity.

or in terms of μ_o and α,

$$C_2 = \mu_o[1 - \alpha \tan^{-1}(\frac{1}{\alpha})] \ . \tag{4.17}$$

The turnaround time is then given by

$$T = 2\mu_o\{\alpha[1 - \pi/4 + \tan^{-1}(\frac{1}{\alpha})] - 1\} \ . \tag{4.18}$$

Within the QSP approximation we may also find the equation of motion during the infall phase. The equation is the same, but the boundary conditions now consist of requiring that μ and $\dot{\mu}$ be continuous at $t = T$. We define the new constants of integration, C_3 and C_4 by

$$\dot{\mu}(t > T) = \frac{1}{2} (\frac{C_3}{\mu^2} + 1)$$

and (4.19)

$$\mu(t > T) - \sqrt{C_3} \tan^{-1} (\frac{\mu}{\sqrt{C_3}}) = \frac{1}{2} (t - T) + C_4 \ .$$

Since $\dot{\mu}(T) = 1$, $C_3 = \mu_T^2$ where $\mu_T \equiv \mu(T)$ is defined by the solution to Equation (4.12) for $0 \leq t \leq T$. Also, since

$$\mu_T - \mu_T\tan^{-1}(1) = C_4 \tag{4.20}$$

we have

$$C_4 = \mu_T(1 - \pi/4) \ . \tag{4.21}$$

The second pair of constants is then related to the first by

$$C_3 = C_1 = \alpha^2\mu_o^2$$

and

$$C_4 = C_2 + \frac{T}{2} = \alpha\mu_o(1 - \pi/4) \; . \qquad (4.22)$$

The entire motion (both ejection and infall phases) is thus determined in the QSP approximation by the parameters α and μ_o, which in turn are specified in terms of the physical parameters ρ, v_a, V_o and M_o. The velocity is shown as a function of time for two combinations of parameters in Figures 4.1 and 4.2.

b) Gravitational limit. In this approximation the (large) mass of the shell is constant. The motion is given by the elementary relation

$$v = V_o - \frac{\Gamma}{R^2} t \qquad (4.23)$$

and the dynamics are unaffected by the accretion flow. Note, however, that the kinetic energy of accretion is still lost to radiation. In this case the turnaround time is $T = V_o R^2/\Gamma$, and the impact time is just twice this value.

Numerical solutions of Equation (4.7) are shown in Figure 4-3 and 4-4. Note that the solutions progress from the gravitational case (v linear in t) to the QSP limit as M_o is reduced. Note also that one effect of the gas flow is to increase the effective escape velocity.

To summarize, we have now developed a description of the velocity of the ejected shell as a function of time. The acceleration phase is determined by processes beyond the scope of this work; accordingly we accept the time scales found in the S4 nova calculations as being correct to within an order of magnitude. The rise times of the outburst to be studied are schematic only. The decay phase, however, can be specified rigorously. The two asymptotic limiting behaviors can be handled analytically. The QSP limit, as illustrated in Figures 4-1 and 4-2, shows a non-linear decrease in the outward velocity. The numerical solutions of the general equation, shown in Figures 4-3 and 4-4, demonstrate the transition from the QSP behavior to the gravitational case, characterized by the familiar linear velocity function (Figure 4-3) and parabolic position function (Figure 4-4), as the initial shell mass is increased. The QSP solution, which is in some sense the more interesting - or at least novel - case, is examined in more detail in Chapter V.

Figure 4-1: Solution to QSP equation of motion for

$M_o = 20 \text{ g cm}^{-2}$

$V_o = 1.5 \times 10^8 \text{ cm s}^{-1}$

$\rho_a = 10^{-9} \text{ g cm}^{-3}$

$M_* = .5\ M_\odot$.

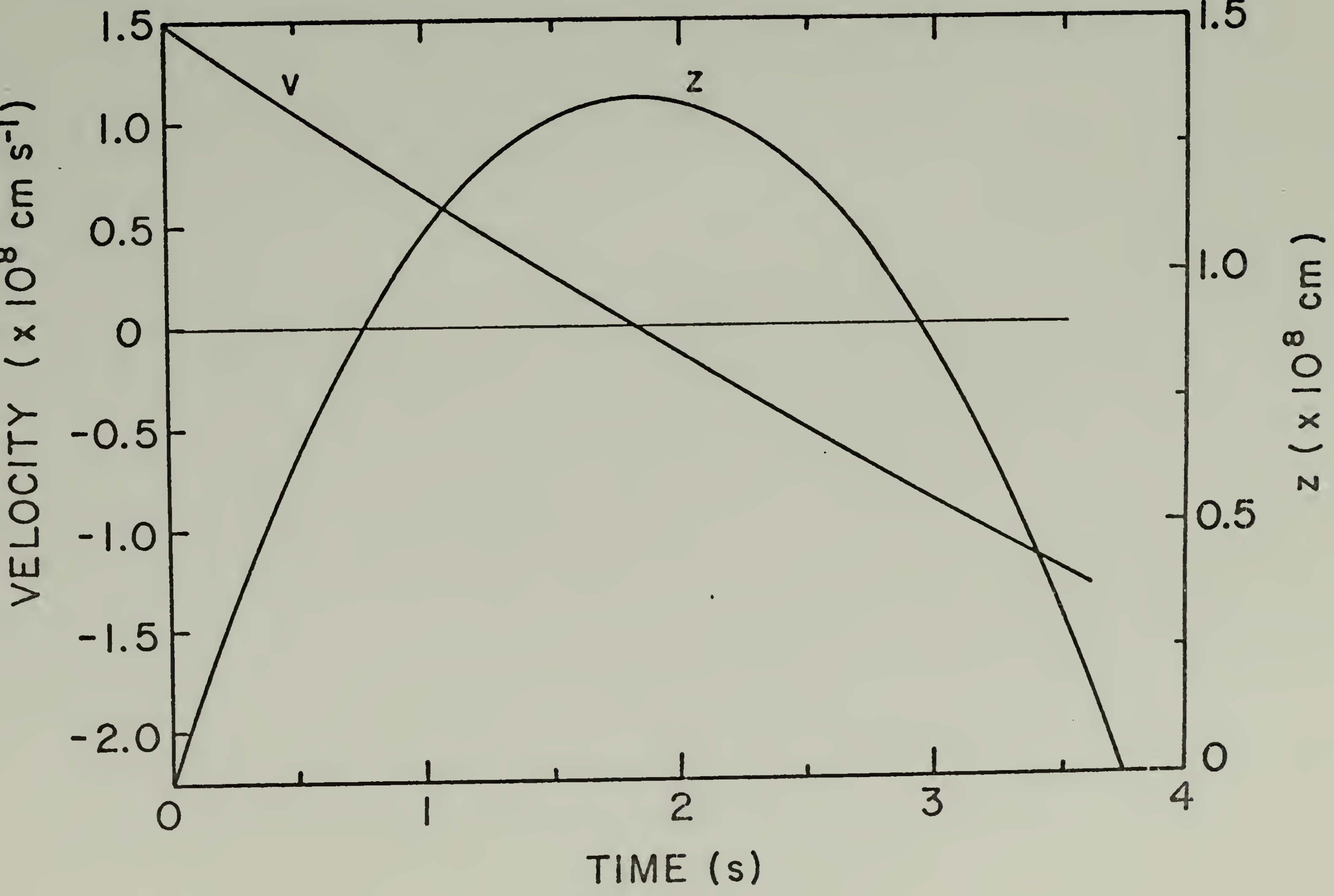
v
z
VELOCITY (x 10^8 cm s^{-1})
1.5
1.0
0.5
0
-0.5
-1.0
-1.5
-2.0
z (x 10^8 cm)
1.5
1.0
0.5
0
TIME (s)
0
1
2
3
4

Figure 4-2: Solution to QSP equation of motion for

$M_o = 20$ g cm^{-2}

$V_o = 3 \times 10^7$ cm s^{-1}

$\rho_a = 10^{-9}$ g cm^{-3}

$M_* = .5\ M_\odot$.

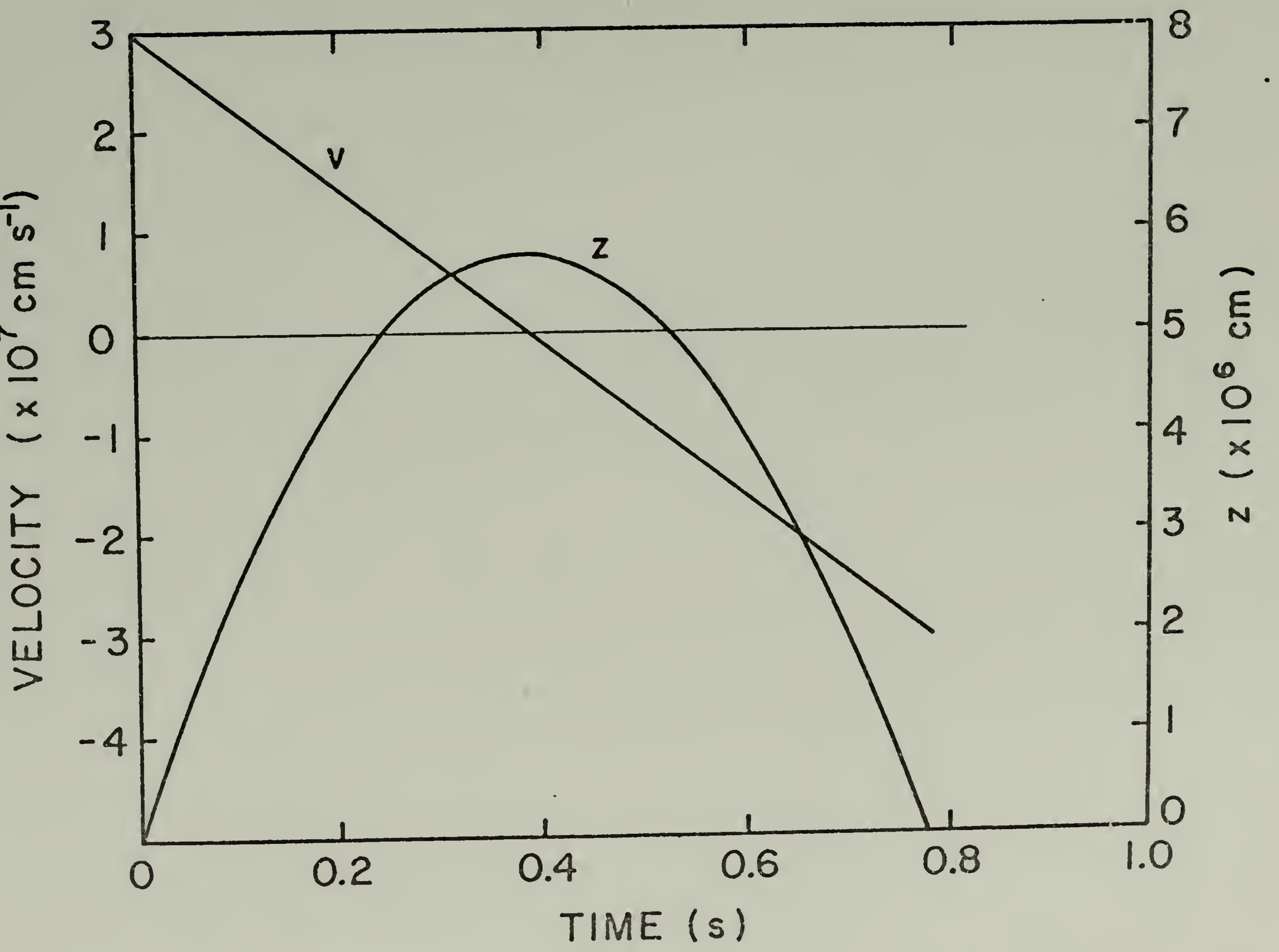
3
2
1
0
-1
-2
-3
-4
VELOCITY (x 10^7 cm s^{-1})
v
z
0
0.2
0.4
0.6
0.8
1.0
TIME (s)
8
7
6
5
4
3
2
1
0
z (x 10^6 cm)

Figure 4-3: Velocity solutions to general equation of motion (4.7) for

$V_o = 3 \times 10^8$ cm s^{-1}

$\rho_a = 10^{-9}$ g cm^{-7}

$M_* = .5\ M_\odot$

M_o as labeled .

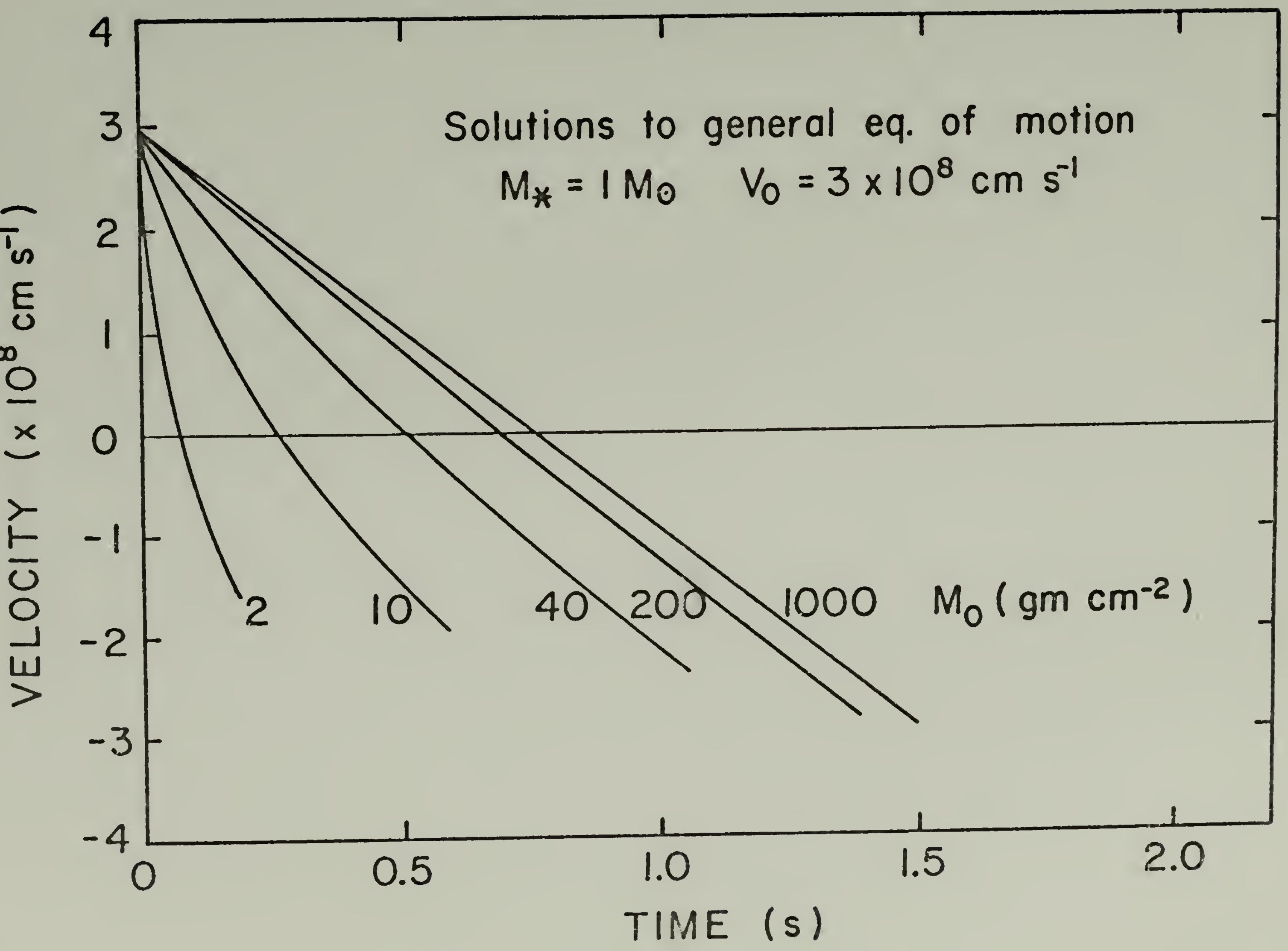
Solutions to general eq. of motion
$M_* = 1\,M_\odot$ $V_0 = 3 \times 10^8$ cm s^{-1}
VELOCITY ($\times 10^8$ cm s^{-1})
4
3
2
1
0
-1
-2
-3
-4
TIME (s)
0
0.5
1.0
1.5
2.0
2
10
40
200
1000
M_0 (gm cm^{-2})

Figure 4-4: Position (height) solutions to general equation of motion (4.7) as in Figure 4-3.

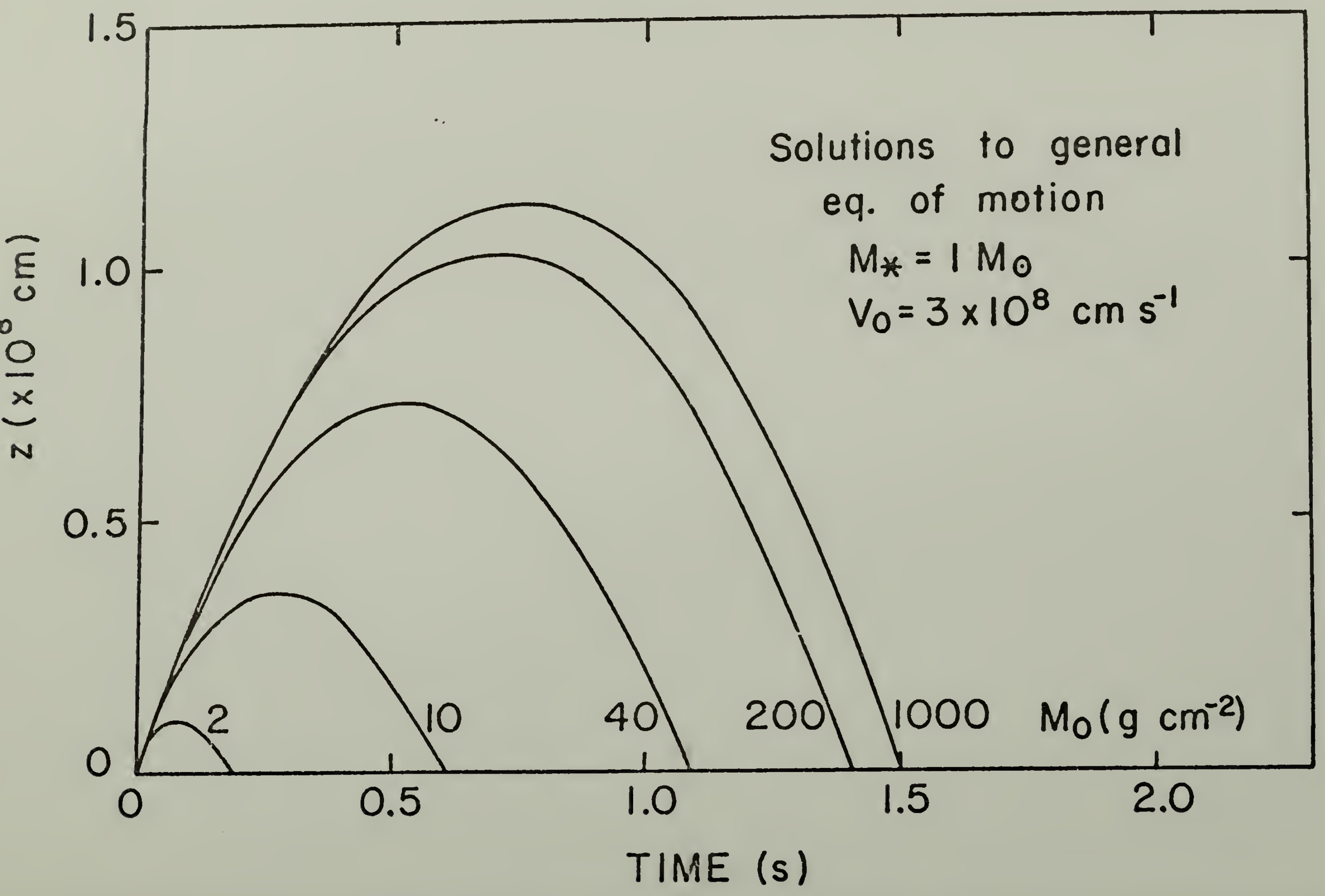
Solutions to general
eq. of motion
$M_* = 1\ M_\odot$
$V_0 = 3 \times 10^8$ cm s^{-1}
z ($\times 10^8$ cm)
1.5
1.0
0.5
0
0
0.5
1.0
1.5
2.0
TIME (s)
2
10
40
200
1000
M_0(g cm^{-2})

CHAPTER V

QSP EQUATION OF MOTION

§1. Solution

In this section we examine in greater detail the QSP limit to the shell motion. Although this requires what are probably rather unusual source parameters, it permits a detailed examination of the effects of the accreting gas per se on the motion of the shell. Since the solution is obtained in analytic form, we can also develop a rigorous expression for the ratio of the shell kinetic energy at impact to the initial shell energy.

For reference purposes the solution to Equation (4.12) and the relevant boundary conditions are summarized as follows:

for $0 \leq t \leq T$, $v = v_a(\dot{\mu} - 1)$

$$\mu - \alpha\mu_o \tan^{-1}\left(\frac{\mu}{\alpha\mu_o}\right) = \frac{1}{2}\, t + \mu_o[1 - \alpha \tan^{-1}(\frac{1}{\alpha})] \; ; \qquad (5.1)$$

for $t \geq T$, $v = v_a(1 - \dot{\mu})$

$$\mu - \alpha\mu_o \tan^{-1}\left(\frac{\mu}{\alpha\mu_o}\right) = \frac{1}{2}\,(t - T) + \alpha\mu_o(1 - \pi/4) \; ; \qquad (5.2)$$

where

$$T = 2\mu_o\{\alpha[1 - \pi/4 + \tan^{-1}(\frac{1}{\alpha})] - 1\} \; . \qquad (5.3)$$

In both regimes

$$\dot{\mu} = \frac{1}{2}\left(\frac{\alpha^2\mu_o^2}{\mu^2} + 1\right) , \quad \mu_o \equiv \frac{M_o}{\rho v_a}$$

$$\alpha \equiv \left[2\,\frac{V_o + v_a}{v_a} - 1\right]^{1/2} \text{ or } V_o = \frac{v_a}{2}(\alpha^2 - 1) \tag{5.4}$$

and at $t = T$, $\mu = \alpha\mu_o$.

We need to derive expressions for the position, z, above the original surface as a function of time (or of μ), the maximum displacement, z_{max}, and the kinetic energy, E_{ki} and time, t_i, at impact ($z = 0$, $t \neq 0$).

The displacement, z, is defined by

$$z = \int_o^t v dt \tag{5.5}$$

and for $0 \leq t \leq$, $v = v_a(\dot{\mu} - 1)$. Thus,

$$z = v_a \int_o^t [\dot{\mu} - 1] dt \tag{5.6}$$

and

$$z = v_a[\mu - \mu_o - t] . \tag{5.7}$$

Substituting for t as a function of μ,

$$z = v_a\{2\alpha\mu_o[\tan^{-1}(\frac{\mu}{\alpha\mu_o}) - \tan^{-1}(\frac{1}{\alpha})] - (\mu - \mu_o)\} . \tag{5.8}$$

Now define a dimensionless variable $\eta \equiv \frac{\mu}{\mu_o}$. Then

$$z = v_a\mu_o\{2\alpha[\tan^{-1}(\frac{\eta}{\alpha}) - \tan^{-1}(\frac{1}{\alpha})] - (\eta - 1)\} . \qquad (5.9)$$

We use the identity

$$\tan^{-1}\{\tan[\tan^{-1}u - \tan^{-1}v]\} = \tan^{-1}(\frac{u - v}{1 + uv})$$

to reduce this to

$$z = v_a\mu_o\{1 - \eta + 2\alpha\tan^{-1}[\frac{\alpha(\eta - 1)}{\alpha^2 + \eta}]\} . \qquad (5.10)$$

The ambiguity in the inverse tangent thus introduced is removed by noting that z = 0 at $\eta = 1$, thus requiring the principal value.

For $T \leq t$ we define z by

$$z = z_{max} - \int_T^t v dt \;, \quad v = v_a(1 - \dot{\mu}) .$$

In this regime

$$t = T + 2\{\mu - \alpha\mu(1 - \pi/4 + \tan^{-1}(\frac{\mu}{\alpha\mu_o}))\} . \qquad (5.11)$$

By the same procedure used for the $0 \leq t \leq T$ regime one finds

$$z_{max} - z = v_a\mu_o\{\eta - \alpha + 2\alpha\tan^{-1}(\frac{\alpha - \eta}{\alpha + \eta})\} . \qquad (5.12)$$

Since, at t = T, $\eta = \alpha$, Equation (5.10) yields

$$z_{max} = v_a\mu_o\{1 - \alpha + 2\alpha\tan^{-1}(\frac{\alpha - 1}{\alpha + 1})\} . \qquad (5.13)$$

We now consider the shell at impact defined by z = 0, $t \neq 0$. Consider Equation (5.12) at z = 0 where $\eta = \eta_i$. This gives

$$z_{max} = v_a \mu_o \{\eta_i - \alpha + 2\alpha \tan^{-1} (\frac{\alpha \quad \eta_i}{\alpha + \eta_i})\} . \tag{5.14}$$

But we already found that (Equation (5.13))

$$z_{max} = v_a \mu_o \{1 - \alpha + 2\alpha \tan^{-1} (\frac{\alpha - 1}{\alpha + 1})\} .$$

We thus require that η_i satisfy the equation

$$\eta_i + 2\alpha \tan^{-1} (\frac{\alpha - \eta_i}{\alpha + \eta_i}) = 1 + 2\alpha \tan^{-1} (\frac{\alpha - 1}{\alpha + 1}) \equiv \phi(\alpha) \tag{5.15}$$

where $\eta_i \neq 1$ since $T_i \neq 0$. Note that, since $\alpha > 1$ by definition for any initial (positive) upward velocity V_o, this equation has a unique solution for each value of α in the regime of interest. Physically, there will be some maximum value of α beyond which the assumptions of constant density and velocity in the accreting gas will no longer hold, and the QSP approximation becomes invalid as herein defined. Solutions giving η_i as a function of α are shown in Figure 5-1. Although the function is nearly linear in the regime illustrated, it rises rapidly for large values of α. This is, however, beyond the scope of the initial assumptions. Note that $\alpha = 1$ implies zero initial velocity, giving the trivial solution $\eta_i = 1$. All other quantities describing the conditions at impact may be derived as functions of η_i and initial conditions.

The time of impact follows immediately from Equation (5.11) and the expression for T, Equation (5.3);

Figure 5-1: Impact mass in units of initial shell mass as a function of initial velocity for given accretion velocity v_a($\alpha \equiv [2 \frac{v_o + v_a}{v_a} - 1]^{1/2}$). Note that this curve is not quite linear. For extremely large values of V_o/v_a (and α) the curve rises more and more steeply. Eventually the approximation breaks down.

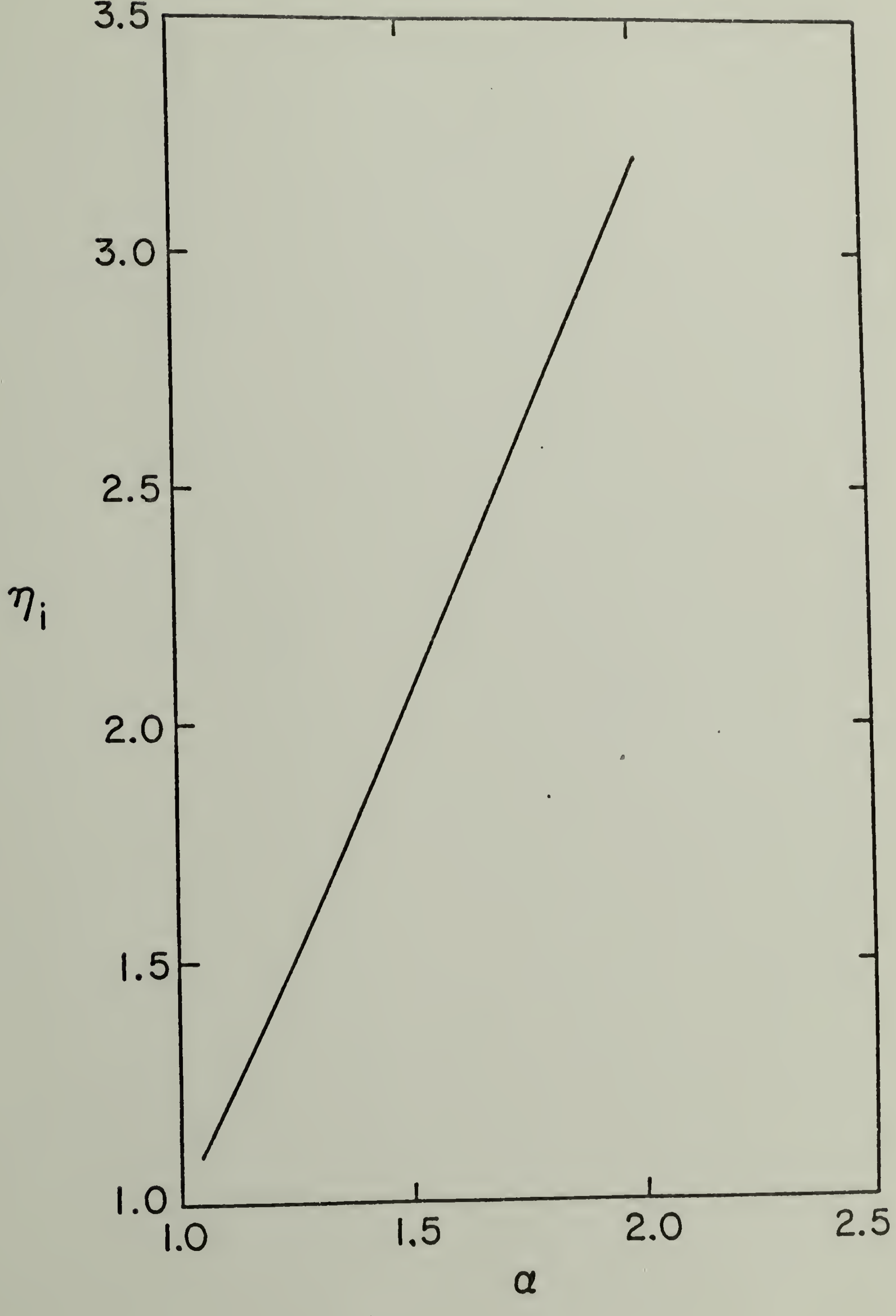
3.5
3.0
2.5
2.0
1.5
1.0
η_i
1.0
1.5
2.0
2.5
α

$$\begin{aligned} T_i &= T + 2\mu_o\{\eta_i - \alpha(1 - \pi/4 + \tan^{-1}(\frac{\eta_i}{\alpha}))\} \\ &= 2\mu_o\{\eta_i - 1 - \alpha \tan^{-1}[\frac{\alpha(\eta_i - 1)}{\alpha^2 + \eta_i}]\} \ . \end{aligned} \qquad (5.16)$$

The velocity during infall is given by

$$v = v_a[1 - \dot{\mu}] = \frac{1}{2} v_a[1 - \frac{\alpha^2}{\eta^2}]$$

so the impact velocity is

$$v_i - \frac{1}{2} v_a[1 - \frac{\alpha^2}{\eta_i^2}] \qquad (5.17)$$

Finally, the kinetic energy per unit area of the shell at impact, E_{ki}, may be determined. The kinetic energy of a unit area of the shell is

$$E_k = \frac{1}{2} \rho v_a \mu v^2 \ .$$

Using the expressions for $\eta_i = \frac{\mu_i}{\mu_o}$ and v_i, we find

$$E_{ki} = \frac{1}{8} \mu_o \rho v_a^2 \eta_i (1 - \frac{\alpha^2}{\eta_i^2})^2 \ . \qquad (5.18)$$

Since we are ultimately interested in the dynamic equilibrium conditions (if they exist) for the shell motion, and the effects of changes in the external parameters (i.e. stability), we need to look at the energy flow during one period P, analogous to the simplified analysis in Chapter III. First note that in the QSP approximation η_i, the ratio of shell mass at impact to shell mass at t = 0, depends only on α, which is a measure of the initial velocity. It is independent of the external density ρ. This is to be understood in terms of the momentum flow during one cycle. The parameter α may be thought of as a measure of the rate of acquisition of momentum per unit mass. Thus the amount of mass flux necessary to stop the shell will depend only on the relative velocities. The rate of acquisition of momentum per second, however, does depend on ρ; and thus so does the value of T_i, the time of impact.

We can define a ratio, R_{EK}, of the shell kinetic energy at impact to that at t = 0. The expression for this is

$$R_{EK} \equiv \frac{E_{ki}}{E_{ko}} = \frac{(\eta_1^2 - \alpha^2)^2}{\eta_i^3(\alpha^2 - 1)^2} . \tag{5.19}$$

Note that this is also independent of ρ. This means that in the QSP approximation a change in the density of the accreting gas does not affect the shell kinetic energy available at impact for a given initial energy. It does affect the duration and spatial amplitude of the motion of the detached shell. In Figure 5-2, R_{EK} is shown as a function of α.

§2. Stability

Since the value of R_{EK} never exceeds 0.4, one might expect the shell motion to damp out, due to a net loss of energy on each cycle. However, there will also be some interval between impact and the

Figure 5-2: Ratio of shell kinetic energy at impact to initial value as a function of initial velocity.

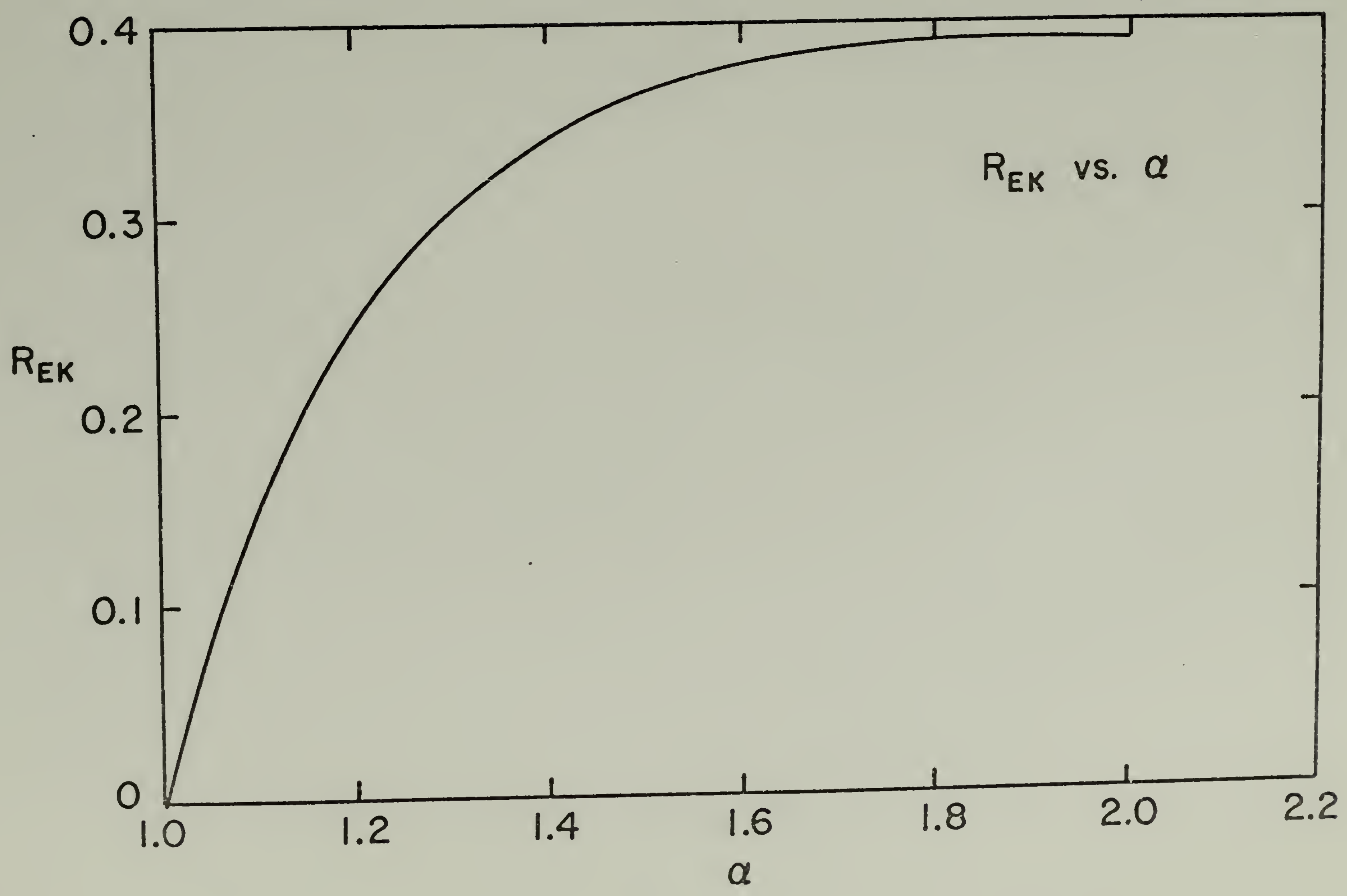
R_{EK} vs. α
R_{EK}
0.4
0.3
0.2
0.1
0
1.0
1.2
1.4
1.6
1.8
2.0
2.2
α

triggering of the next cycle, during which the gas in the outer layers of the star is compressed and heated. During this interval the star will continue to acquire kinetic energy from the accretion flow. Although the details of the transport of this energy into the compressing layers are quite complicated, we must take this into account in order to find a steady state description of the oscillations. We do this by making the following rather crude assumption: we take the total energy available for compression to be given by

$$E_c = E_{ki} + \varepsilon \frac{dE_a}{dt} (\tau_c) \qquad (5.20)$$

where $\frac{dE_a}{dt}$ is the (constant) rate of deposition of kinetic energy by the accreting gas. τ_c is the duration of the compression, and ε is some efficiency factor in which are buried the details of the transport phenomena.

In equilibrium the compression time is the difference between the period and the sum of the time during which the shell is detached (T_i for $t = 0$ defined as the end of the acceleration phase) plus the rise time. Since the rise time is small compared to the others it may be neglected. For the system to be in equilibrium the kinetic energy of the shell which is lost to radiation must be balanced by the energy gained from the accretion flow during infall and compression. We are thus treating the thermonuclear burning phase as a means of converting accretion energy into shell energy and then into radiation. This approach allows us to write down the equilibrium relation between P, ρ and α given by

$$E_c = E_{ki} + \frac{1}{2}\rho v_a^3(P - T_i)$$

or

$$R_{EK} + \varepsilon \frac{\frac{1}{2}\rho v_a^3}{E_{ko}}(P - T_i) = 1 \ . \qquad (5.21)$$

Inserting the expressions for R_{EK} and T_i in terms of α and μ_o, we can solve for P;

$$P^* = 2\mu_o\left[\frac{2}{\varepsilon}\left\{(\alpha^2 - 1)^2 - \frac{(\eta_i^2 - \alpha^2)^2}{\eta_i^3}\right\} + \left\{\eta_i - 1 - \alpha\tan^{-1}\left[\frac{\alpha(\eta_i - 1)}{\alpha^2 + \eta_i}\right]\right\}\right] , \qquad (5.22)$$

where P* indicates the equilibrium period. Note that the only dependence on ρ is through $\mu_o = \frac{M_o}{\rho v_a}$, which has been separated. In Figure 5-3 the function $\frac{P^*}{\mu_o}$ has been plotted for the range of interest in α, assuming $\varepsilon = \frac{1}{10}$.

We can now consider the question of what happens if $P \neq P^*$. Suppose that $P = P^* \pm \delta P$. We then have

$$\frac{E_c}{E_{ko}} = \frac{(\eta_i^2 - \alpha^2)^2}{\eta_i^3(\alpha^2 - 1)^2} + \frac{\varepsilon}{4\mu_o(\alpha^2 - 1)^2}[P^* \pm \delta P - T_i] \qquad (5.23)$$

or from Equation (5.24),

$$\frac{E_c}{E_{ko}} = 1 \pm \frac{\varepsilon}{4\mu_o(\alpha^2 - 1)^2}\delta P \ . \qquad (5.24)$$

Since the denominator in the last term is positive definite, this says that $\frac{E_c}{E_{ko}}$ varies directly as δP.

The value of E_c/E_{ko} on a given cycle determines the value of E_{ko} on the next cycle; if the thermonuclear "spring" is over or under compressed with respect to equilibrium, it will increase or decrease the burn rate (Cameron 1966) and thus the value of E_{ko}. Assuming that the burn depth (and thus M_o) remains constant, this means that for $E_c/E_{ko} > 1$, α increases and for $E_c/E_{ko} < 1$, α decreases.

If α changes from one cycle to the next, so will the value of P*. Since P* is a monotonically increasing function of α (Figure 5-3), the new value of P* will be such as to reduce δP. We thus find that the period equilibrium is stable, but will reflect systematic changes in α.

We also wish to investigate the response of the system to changes in ρ, the external density. From Equation (5.27) and the definition of μ_o, we may write

$$P^* = \frac{M_o}{v_a} \frac{F(\alpha)}{\rho} , \tag{5.25}$$

implicitly defining $F(\alpha)$. A change in density, $\delta\rho$, thus produces a change in the equilibrium period, δP^*, given by

$$\frac{\delta P^*}{P^*} = - \frac{\delta\rho}{\rho} . \tag{5.26}$$

Any systematic change in the density will thus produce a systematic change in the equilibrium period; an effect observed in some periodic x-ray sources.

Figure 5-3: Equilibrium period in units of μ_o (see text) as a function of the initial velocity parameter α.

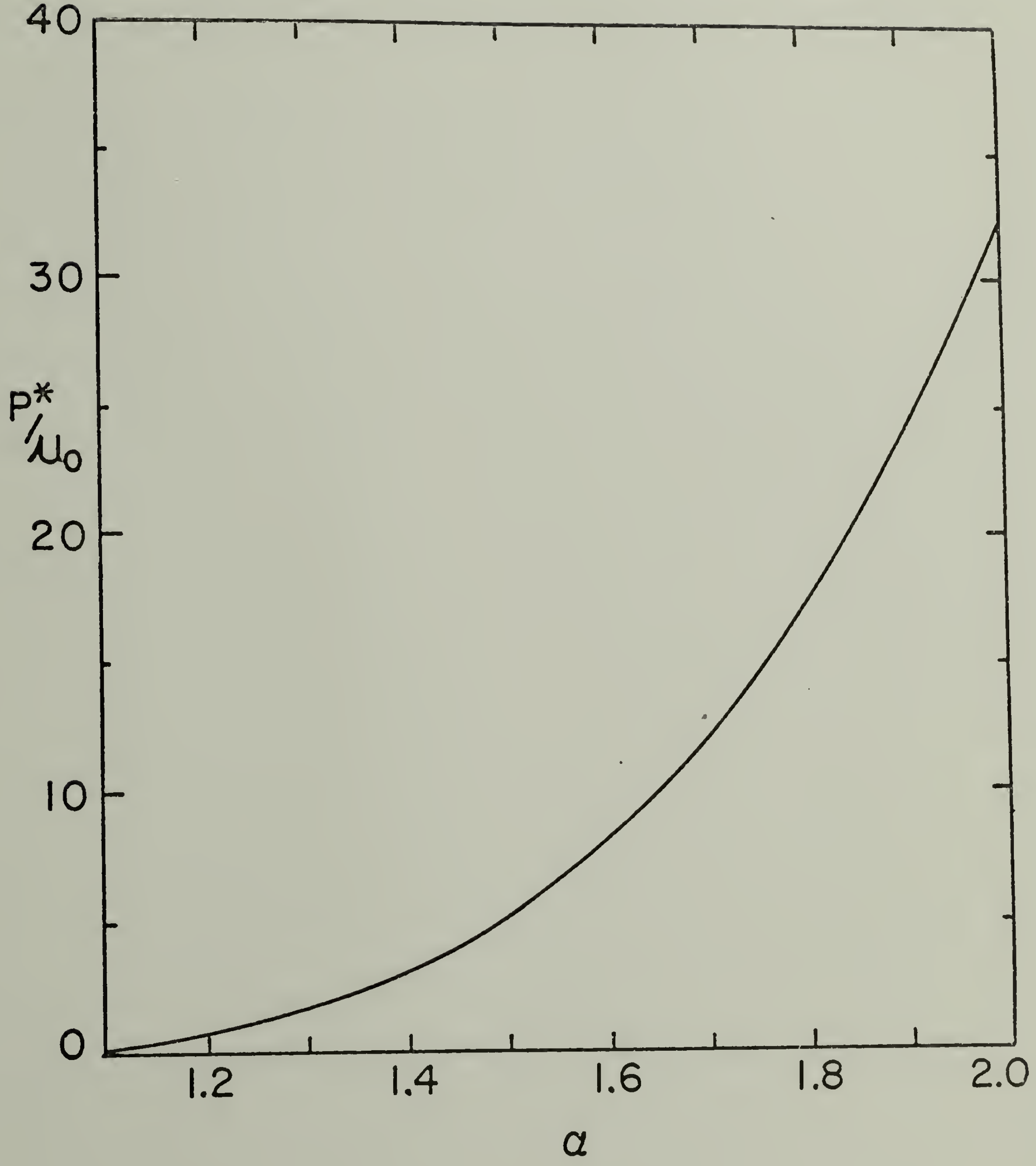
40
30
20
10
0
P*/u0
1.2
1.4
1.6
1.8
2.0
α

Rather than assuming a constant value for M_o, an alternative approach is to assume that the thermonuclear shell is triggered at a more or less constant energy level whenever the energy of compression passes some threshold value. This amounts to assuming a constant value for the product M_oV_o, the momentum per unit area.

This implies that

$$\mu_o\alpha \equiv \frac{\phi_o}{\rho} \ ; \quad \phi_o = \text{const.} \tag{5.27}$$

The assumption of a constant (threshold) compression energy, E_{th}, then implies that

$$E_{th} = E_{ki} + \varepsilon \frac{1}{2} \rho v_a^3 (P - T_i)$$

or (5.28)

$$P^* = \frac{E_{th} - E_{ki}}{\frac{1}{2} \rho v_a^3} + T_i \ .$$

Substituting for E_{ki}, T_i we have

$$P^* = \frac{E_{th}}{\frac{1}{2} \rho v_a^3} + 2\mu_o \{\eta_i - 1 - \alpha \tan^{-1} [\frac{\alpha(\eta_i - 1)}{\alpha^2 + \eta_i}] - \frac{1}{8} (\eta_i (1 - \frac{\alpha^2}{\eta_i^2})^2)\} \tag{5.29}$$

Separating the density dependence (and using Equation (5.27)),

$$P^* = \frac{1}{\rho} [2 \frac{E_{th}}{v_a^3} + \frac{2\phi_o}{\alpha} \{\eta_i - 1 - \alpha \tan^{-1} [\frac{\alpha(\eta_i - 1)}{\alpha^2 + \eta_i}] - \frac{1}{8} \frac{(\eta_i^2 - \alpha^2)^2}{\eta_i^3}\}] \tag{5.30}$$

where again $P^* \propto \frac{1}{\rho}$, and the efficiency factor ε has been neglected. This is written as

$$P^* = \frac{1}{\rho}\left(\frac{2E_{th}}{v_a^3} + 2\phi_o G(\alpha)\right) . \tag{5.31}$$

The function G(α) (and thus, to within a constant and a scale parameter, P*) is plotted vs α in Figure 5-4. Since it is again monotonic, the general stability arguments above may be directly applied.

§3. Summary

We have found that, for the QSP limit, the fraction of the initial shell energy returned is a function of the initial velocity only, and never exceeds 0.4. We have also argued from this that, for constant initial mass, the period between outbursts should be neutrally stable against changes in accretion density and ejection velocity. If we instead allow M_o to vary, but assume a constant threshold value of the compression energy (which amounts to a critical temperature and density in the burning layer), the period should also have neutral stability.

Figure 5-4: The function $G(\alpha)$ (see text).

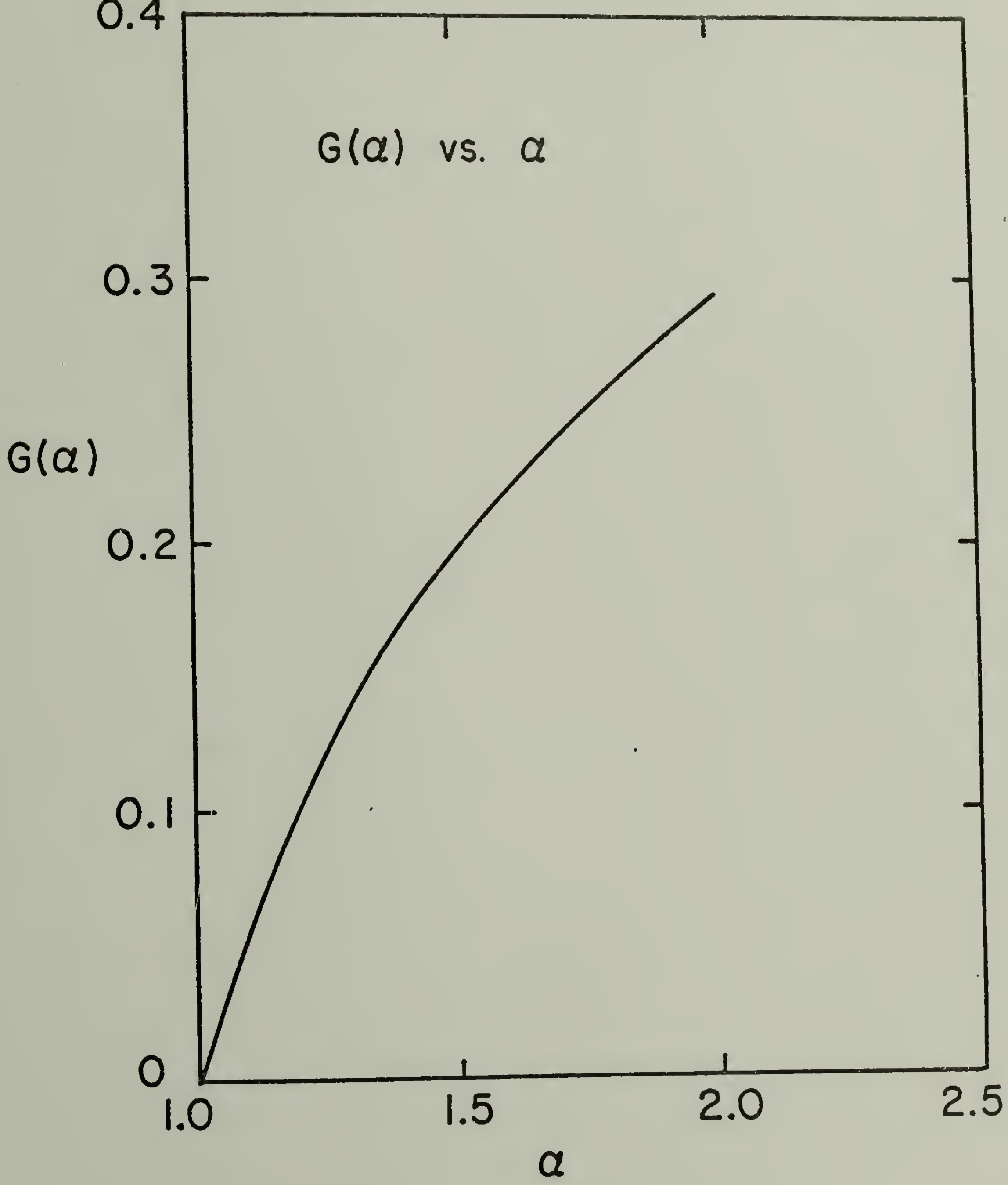
G(α) vs. α
G(α)
0.4
0.3
0.2
0.1
0
1.0
1.5
2.0
2.5
α

QSP Solution

Table of Impact Conditions

(note that all quantities are functions of α, μ_o, ρ, v_a only)

1) $\eta_i \equiv \frac{\mu_i}{\mu_o}$ is defined by

$$\eta_i + 2\alpha \tan^{-1}\left(\frac{\alpha - \eta_i}{\alpha + \eta_i}\right) = C_\alpha$$

where

$$C_\alpha \equiv 1 + 2\alpha\left(\frac{\alpha - 1}{\alpha + 1}\right)$$

and

$$\eta_i \neq 1 \; .$$

2) $v_i = \frac{1}{2} v_a\left[1 - \frac{\alpha^2}{\eta_i^2}\right]$.

3) $T_i = T + 2\mu_o\{\eta_i - \alpha(1 - \pi/4 + \tan^{-1}(\frac{\eta_i}{\alpha}))\}$

and

$$T = 2\mu_o\{\alpha[1 - \pi/4 + \tan^{-1}(1/\alpha)] - 1\} \; .$$

4) $E_{ki} = \frac{1}{8} \mu_o v_a^3 \rho \eta_i \left(1 - \frac{\alpha^2}{\eta_i^2}\right)^2$

at

$t = T$, $R = R_{max}$

$$R_{max} = v_a \mu_o\{1 - \alpha + 2\alpha \tan^{-1}\left(\frac{\alpha - 1}{\alpha + 1}\right)\} \; .$$

CHAPTER VI

LIGHT CURVES AND SPECTRA

Having developed both the radiation analysis and the velocity curves for the shell, we can now combine them to investigate the source luminosity as a function of time. Along with the "pulse shapes" thus produced, one can also see the time development of the spectrum of the source. In all of the computed curves, the leading edge of the peak is schematic only. The time scale for the pulse rise should be correct to within a factor of two or three, as outlined in Chapter IV, but the linearity is assumed rather than derived. The curves are parameterized in terms of the "initial" (maximum) velocity, and the decay phase is computed according to the relevant treatment of the velocity development.

In order to minimize the number and complexity of the figures, a specific value of the stellar mass, .5 $M_\odot$, is assumed, which implies a stellar radius, R_*, of about 1.0 x 10^9 cm. This is taken from the M vs R relation for cold white dwarfs as given in Schwartzschild (1958). A white dwarf undergoing the evolutionary stages of mass transfer and heating leading to the assumed detonation is likely to be somewhat larger for a given mass than its cold, unperturbed counterpart. A single value has also been assumed for the density of the accretion flow, $\rho_a = 10^{-9}$ g cm^{-3}. The luminosities are per unit area in CGS units; within the assumption of a plane parallel radiating layer they are thus to be multiplied by the surface area to give total luminosities.

The general case is illustrated in Figures 6-1 and 6-2. These are obtained using numerical solutions of the general equation of motion (Equation 4.7); Figure 6-1 illustrates the approach to the gravitational limit. The curves are plotted to illustrate the effects of the initial mass and peak velocity parameters. It is apparent that, while both parameters affect the shape of the pulse, the overall duration is most strongly affected by the initial shell velocity. The "spikiness" increases as the initial velocity increases and as the initial mass decreases. The instantaneous luminosity, of course, depends only on the velocity.

These figures schematically illustrate a problem in comparing computed curves with observed pulse shapes. In observational data there is always some constant signal underlying the pulse, either due to a constant component in the source, or to the general background. The level of this constant component can drastically change the pulse shape. The dashed line in these figures represents the luminosity of a standing shock. While this is not intended to represent a minimum luminosity (since clearly during the infall phase the velocity of the shell is negative, and the luminosity below the standing shock level), it is unlikely that the luminosity between peaks will be much below this level. Under appropriate circumstances and compression time scales, this could produce a post-peak dip below the unpulsed level, or it could hide the presence of a low luminosity tail on the peak.

Figures 6-3, 6-4, and 6-5 illustrate the limiting cases of the shell motion. While there is overall similarity in the sets of curves,

Figure 6-1: Light curves for the general Equation (4.7) with $V_o = 3 \times 10^8$ cm s^{-1} and various values of M_o. Stellar mass is .5 $M_\odot$ and $\rho = 10^{-9}$ g cm^{-3}.

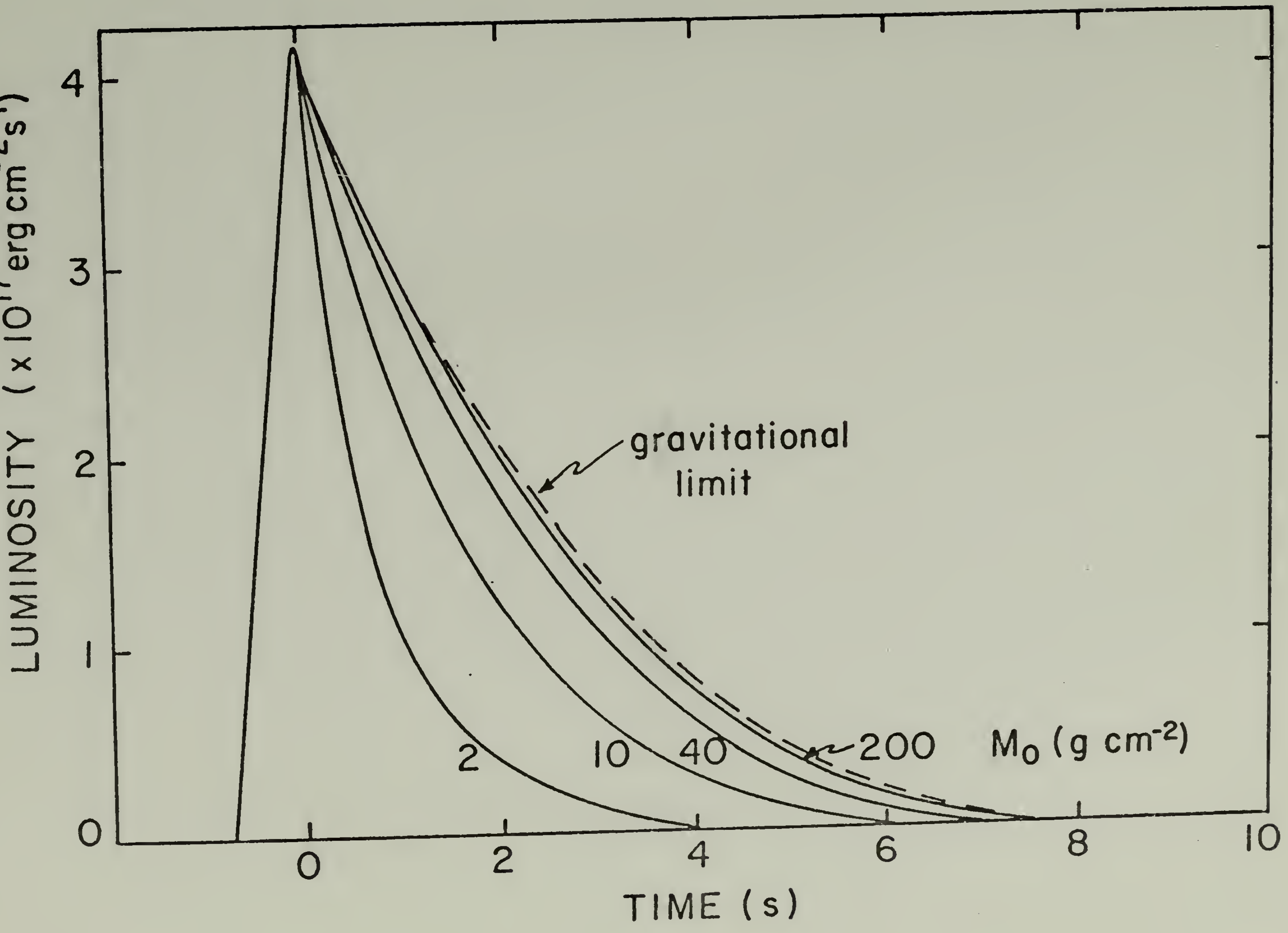
LUMINOSITY $(\times 10^{17}\ \mathrm{erg\ cm^{-2}\ s^{-1}})$
0
1
2
3
4
TIME (s)
0
2
4
6
8
10
gravitational limit
2
10
40
200
M_0 (g cm^{-2})

Figure 6-2: Light curves for the general equation with $M_o = 20$ g cm^{-2} and various values of V_o. Same stellar and accretion parameters as in 6-1.

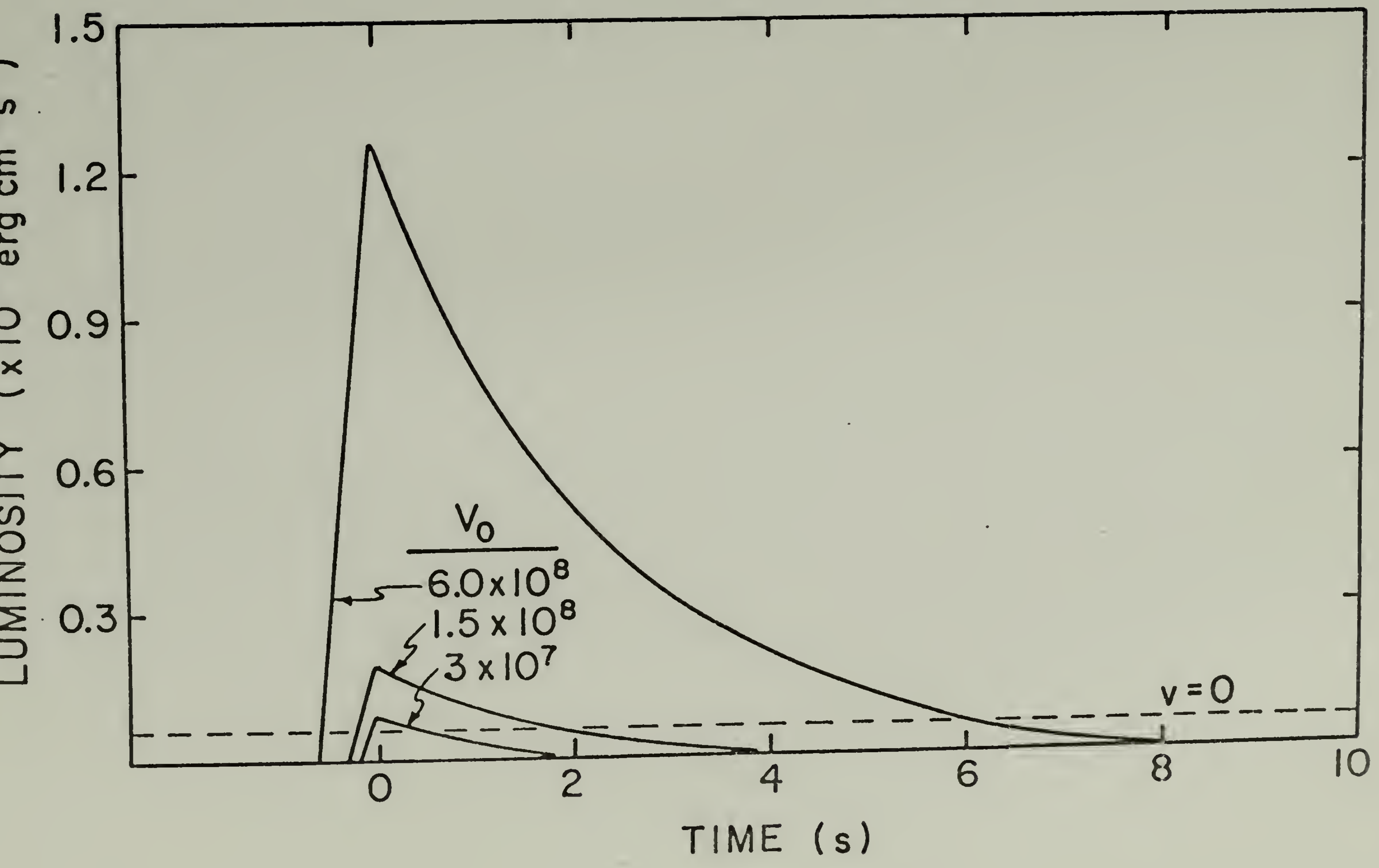

LUMINOSITY (x 10^{18} erg $cm^{-2}s^{-1}$)
1.5
1.2
0.9
0.6
0.3
V_0
6.0×10^8
1.5×10^8
3×10^7
v = 0
0
2
4
6
8
10
TIME (s)

Figure 6-3: Gravitational limit light curves for various values of V_o and stellar mass .5 $M_\odot$.

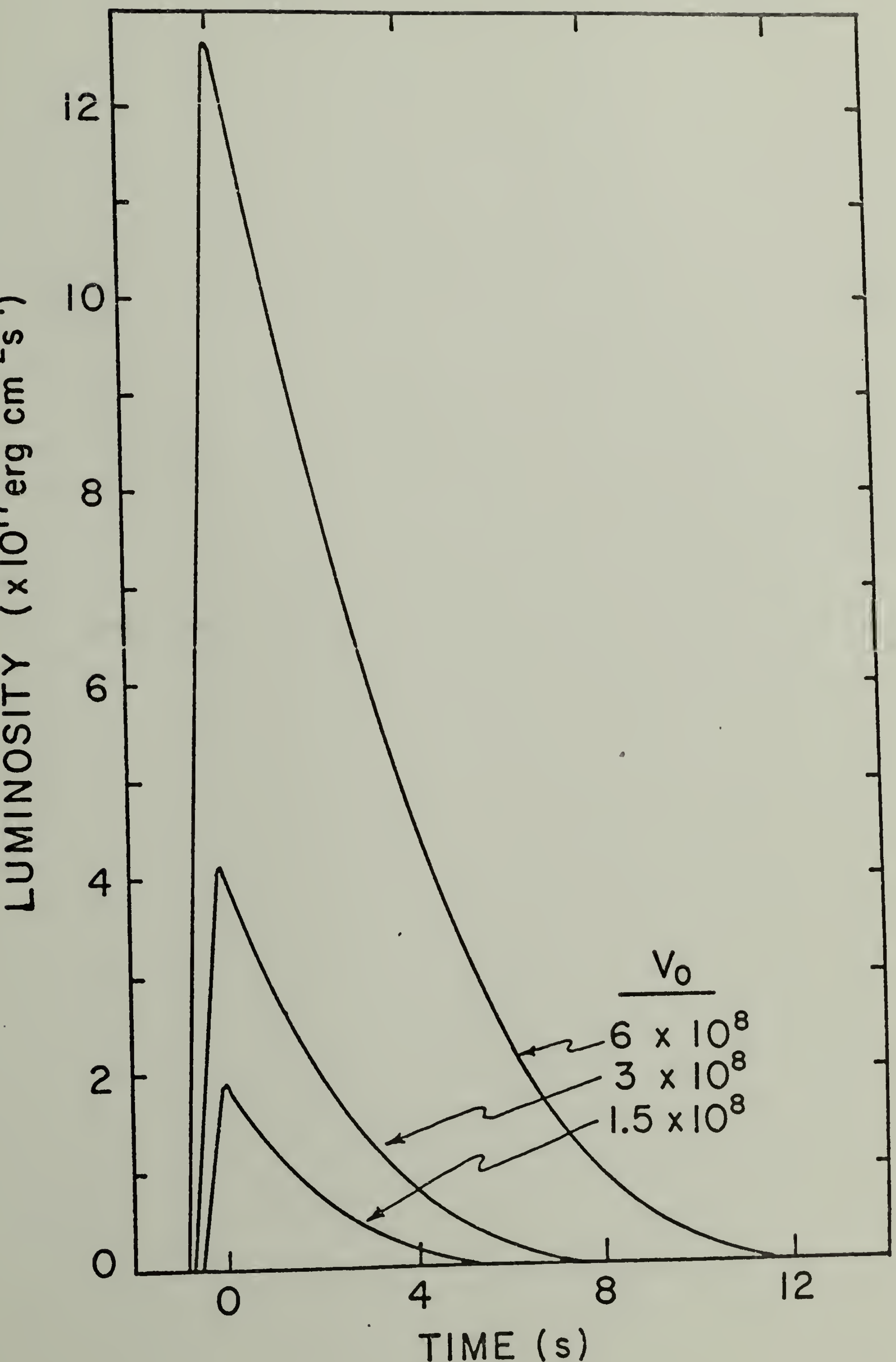
LUMINOSITY (x 10^{17} erg cm^{-2}s^{-1})
0
2
4
6
8
10
12
TIME (s)
0
4
8
12
V_0
6 x 10^8
3 x 10^8
1.5 x 10^8

Figure 6-4: QSP limit light curves for $v_a = 3 \times 10^8$ cm s^{-1}, $V_o = 3 \times 10^8$ cm s^{-1} and various values of M_o.

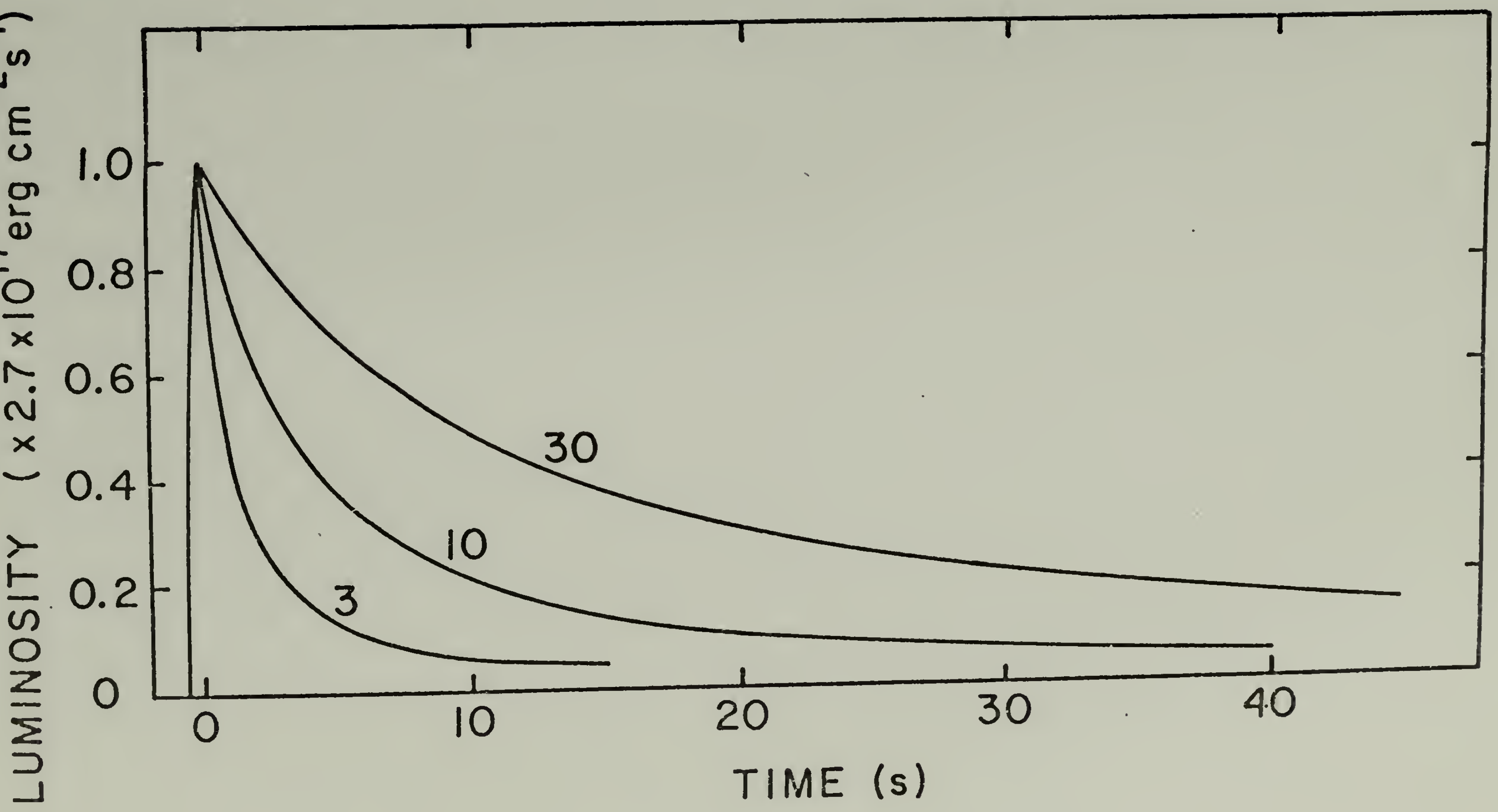

LUMINOSITY (x 2.7 x 10^17 erg cm^-2 s^-1)
1.0
0.8
0.6
0.4
0.2
0
30
10
3
0
10
20
30
40
TIME (s)

Figure 6-5: QSP limit light curves for $v_a = 3 \times 10^8$ cm s^{-1}, $M_o = 20$ g cm^{-2} and various values of V_o.

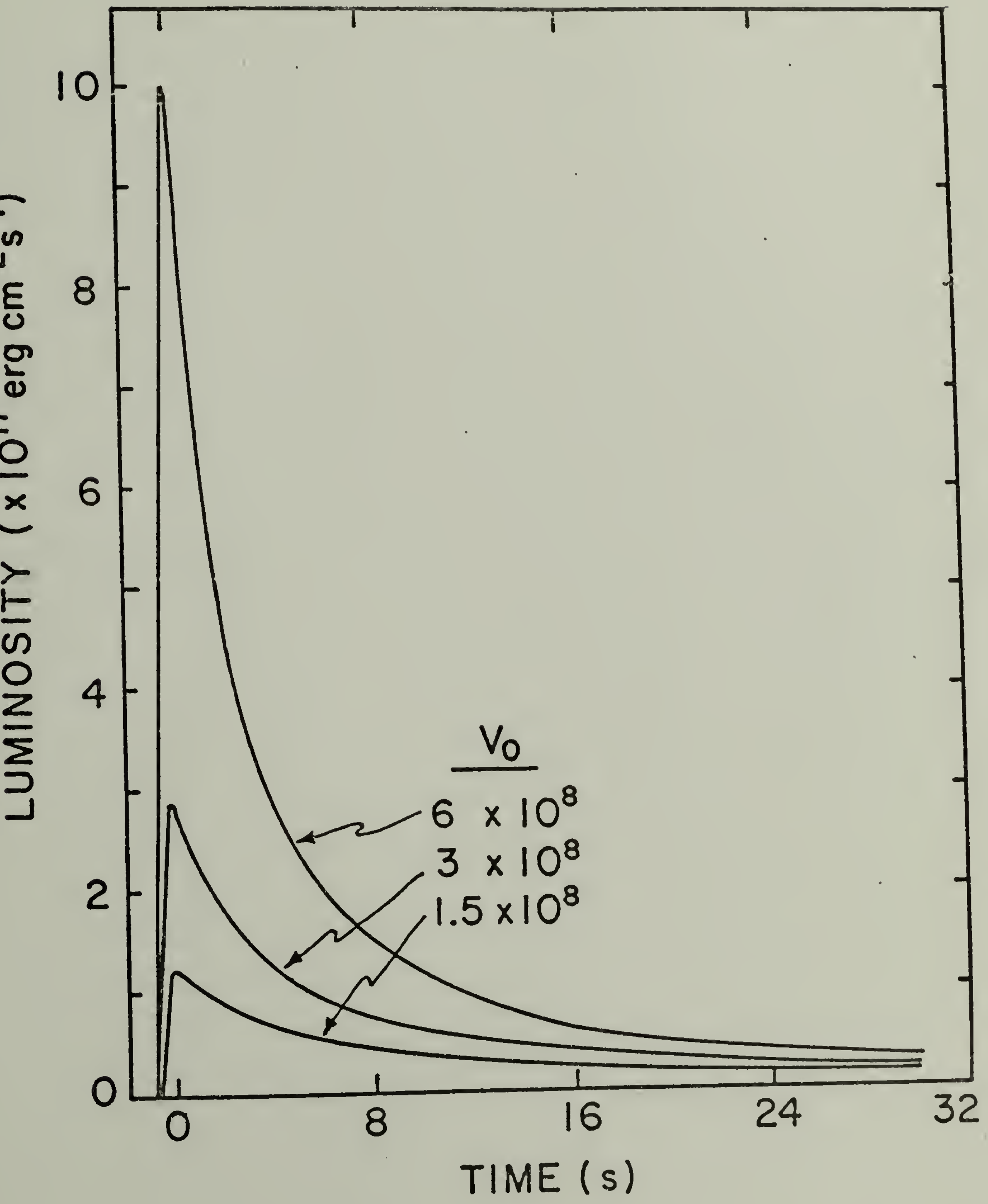
LUMINOSITY (x 10^17 erg cm^-2 s^-1)
10
8
6
4
2
0
0
8
16
24
32
TIME (s)
V0
6 x 10^8
3 x 10^8
1.5 x 10^8

there are also distinctive trends. In particular, the QSP curves show a much more prominent and persistent tail than those for the gravity limit. This reflects the fact that the downward acceleration of the shell is velocity dependent in the QSP case, but constant in the gravitational case. In fact, examination of the QSP solution shows that the limiting downward velocity is one half of the accretion velocity.

The semi-logarithmic plots in Figures 6-6 and 6-7 illustrate an even more striking difference in the decay portions of the peaks. The QSP curves are steeper than exponential; i.e. if an exponential is fitted to the latter portion of the curve, the peak will be above the fitted function. For the gravitational case, however, the peak will always be below a function fitted in the same way. Since a number of attempts have been made to fit the observed behavior of x-ray sources, especially burst sources, in just this way, one can hope to use the functional form of the decay phase to determine which regime is applicable for sources to which this model is applied. This, in turn, should yield at least a limit on the ratio of the initial shell mass to the accretion density.

Perhaps the most characteristic behavior of this model is the time development of the x-ray spectrum. As was shown in Chapter III, the instantaneous spectrum can be quite close to that of a homogeneous thermal source. However, any real observation will be integrated over some finite time span, and this will complicate the spectral analysis. The general behavior expected is a monotonic decrease in the effective

Figure 6-6: Same as Figure 6-5 on a semi-log scale illustrating the shape of the decay phase.

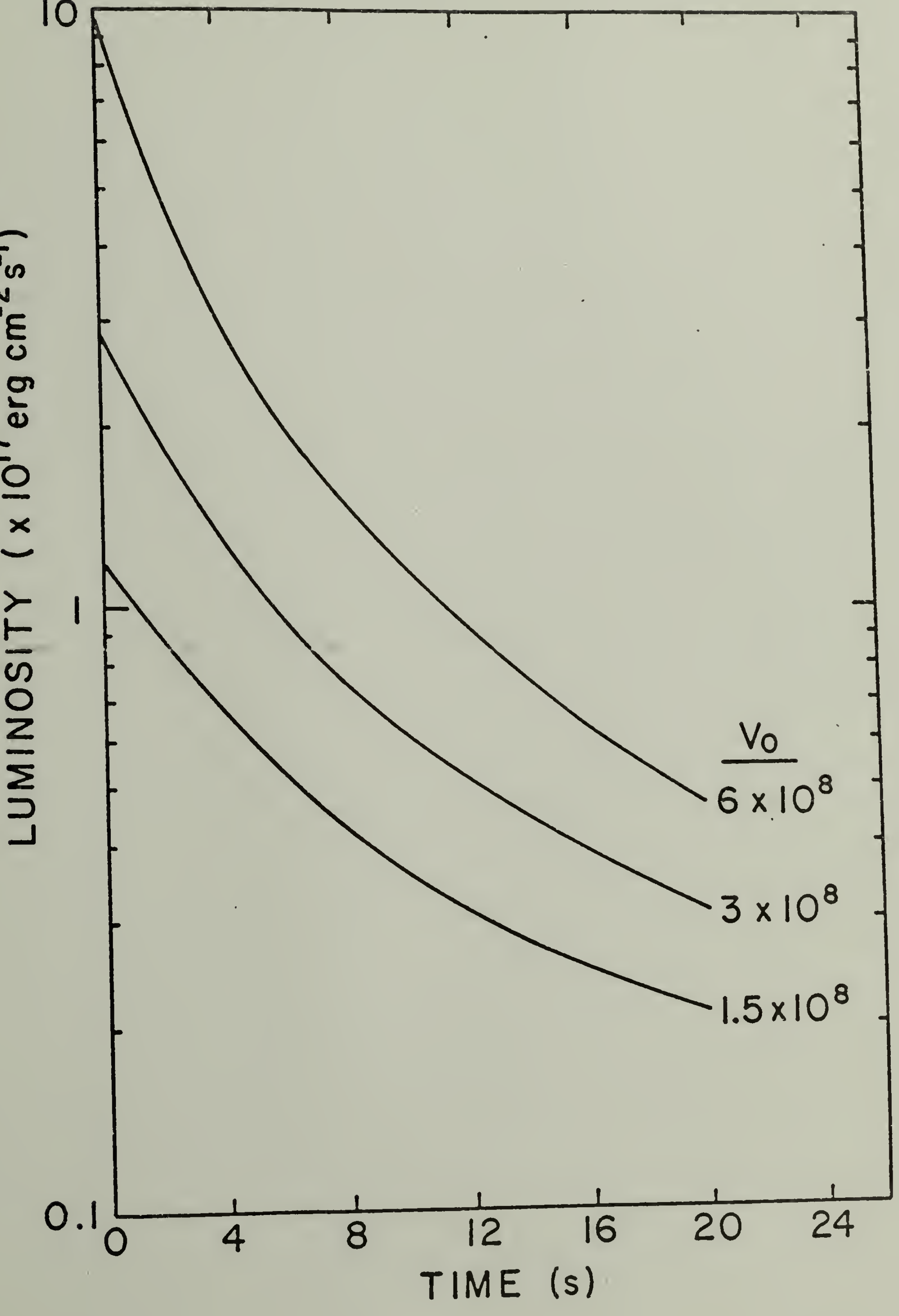
10
1
0.1
LUMINOSITY (x 10^{17} erg cm^{-2} s^{-1})
0
4
8
12
16
20
24
TIME (s)
V_0
6×10^8
3×10^8
1.5×10^8

Figure 6-7: Same as Figure 6-3 on a semi-log scale illustrating the shape of the decay phase (compare to Figure 6-6).

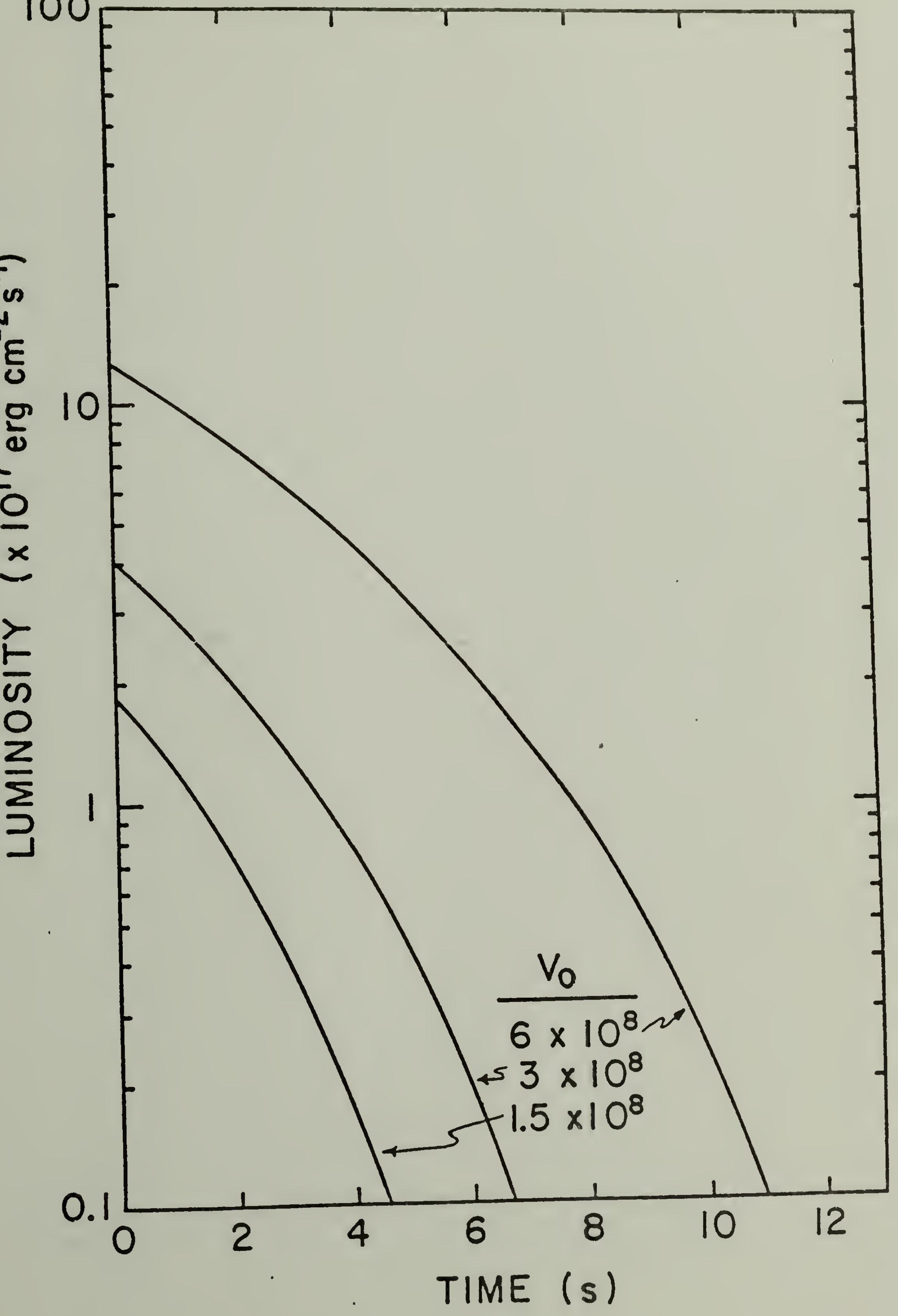

100
10
1
0.1
LUMINOSITY (x 10^{17} erg cm^{-2} s^{-1})
0
2
4
6
8
10
12
TIME (s)
V$_0$
6 x 10^8
3 x 10^8
1.5 x 10^8

temperature, but the use of a single best-fit temperature becomes less appropriate as the integration time increases. An alternative is the use of a hardness ratio, as in Lewin et al. (1976). This can be defined as the ratio of the counts in some high energy band to those in some low energy band, with the bands being chosen arbitrarily according to the detectors involved. For the present purpose we have used the definitions of the SAS-3 group, where the hardness ratio, HR, is defined as the ratio of the flux from 6 to 10 KeV to the flux from 2 to 6 KeV. For this choice HR = 1 would be appropriate to a power law of index 0.25, or a thermal spectrum at 2×10^8 K with a low energy cutoff at 3 KeV (Clark et al. 1976). The curves displayed in Figure 6-8 have been computed using a half-second integration time, and no low energy cutoff. Without a cutoff the 2×10^8 K temperature would correspond to a hardness ratio of ~ .57, including the energy dependence of the Gaunt factor.

Figure 6-9 shows the general relation between the luminosity per unit area and the velocity. It is very close to the relation one might naively expect from the assumption that the kinetic energy is instantaneously lost to radiation, i.e.

$$L = \frac{1}{2} \rho v^3$$

where v is the sum of the accretion velocity and the shell velocity. In fact, the curves deviate slightly from a pure cubic in v. Two values for the density are plotted to illustrate that L does scale linearly with ρ.

Figure 6-8: Hardness ratio vs time for

A - general equation,

$M_* = .5\ M_\odot$

$\rho = 10^{-9}\ \mathrm{g\ cm^{-3}}$

$V_o = 6 \times 10^8\ \mathrm{cm\ s^{-1}}$

$v_a \simeq 3.7 \times 10^8\ \mathrm{cm^{-1}}$.

B - general equation as in A but with

$V_o = 1.5 \times 10^8\ \mathrm{cm\ s^{-1}}$.

C - QSP limit,

$V_o = 6 \times 10^8\ \mathrm{cm\ s^{-1}}$

$v_a = 3 \times 10^8\ \mathrm{cm\ s^{-1}}$.

D - same as C except,

$V_o = 1.5 \times 10^8\ \mathrm{cm\ s^{-1}}$.

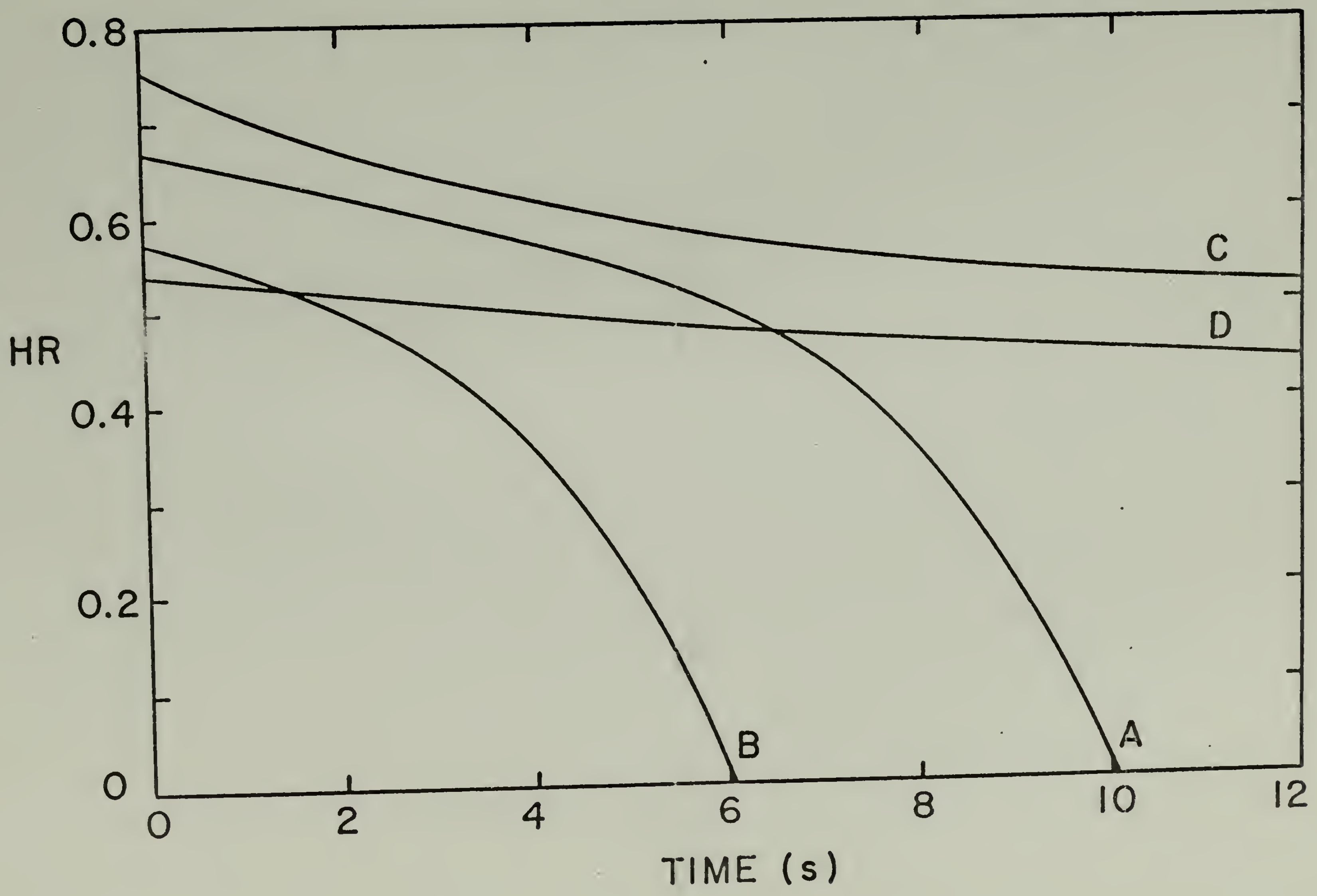
0.8
0.6
HR
0.4
0.2
0
0
2
4
6
8
10
12
TIME (s)
A
B
C
D

Figure 6-9: Luminosity per unit area as a general function of the relative velocity v for two values of the accretion density, ρ.

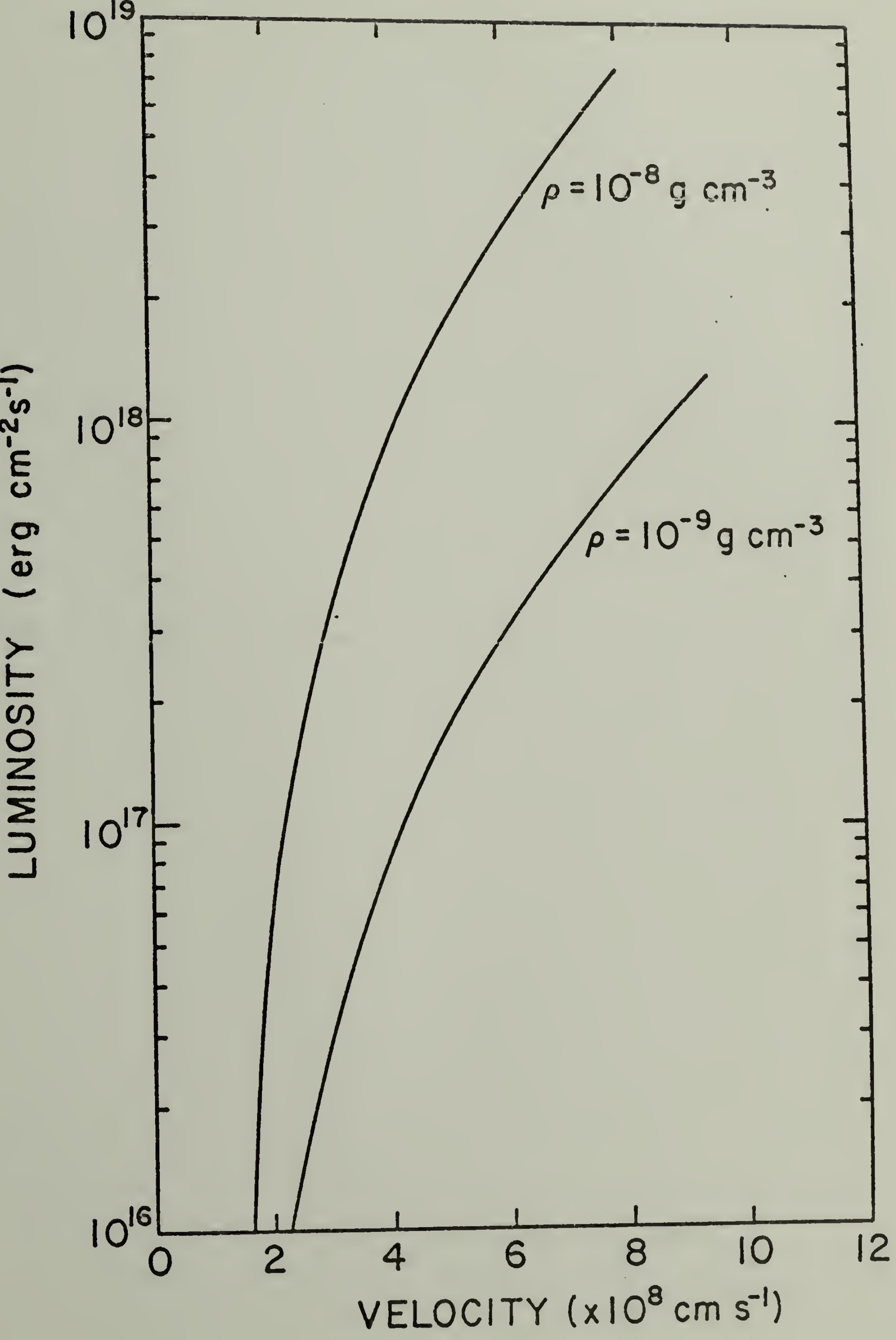

LUMINOSITY (erg cm^{-2}s^{-1})
10^{19}
10^{18}
10^{17}
10^{16}
$\rho = 10^{-8}$ g cm^{-3}
$\rho = 10^{-9}$ g cm^{-3}
0
2
4
6
8
10
12
VELOCITY (x10^{8} cm s^{-1})

CHAPTER VII

DISCUSSION AND CONCLUSION

We are now in a position to consider the large astronomical question involved here: having concluded that white dwarf x-ray sources should exist, what do they look like and can this type of model explain any known x-ray sources? We will first examine some of the general hallmarks of the models, and then consider similarities between the model predictions and some known sources. Finally, since the model investigated here is quite simplified, we will consider the changes to be expected if some of the simplifying assumptions are relaxed.

A single outburst is characterized by a rather sharp peak, and except for initial velocities quite small compared to the accretion velocity is generally asymmetric with the mean slope of the trailing edge somewhat less steep than that of the leading edge. The overall duration of the outburst ranges upward from several tenths of seconds to several tens of seconds, with the longer pulses having generally a more pronounced low intensity tail. The shape of this decay phase is controlled by the mass in the ejected shell for a given stellar mass and accretion density.

The decay is accompanied by a softening of the emitted spectrum. Expressed in terms of hardness ratio the spectrum declines approximately linearly in time for most of the duration of the decay, after a rapid rise. The values of the hardness ratio for the SAS-III energy bands lie in the range .3 to .8.

For the QSP limit the hardness ratio also has a short period of rapid decline preceding the linear regime, while in the gravitational limit there is a rapid decline following the linear region. Because of the way in which hardness ratio is defined it is not possible to determine a specific maximum temperature from a single value of the hardness ratio unless there is additional information as to the presence or absence of a low energy cutoff. Fortunately this can be obtained to some extent by examining the individual low-energy channels. For a source in which the maximum temperature at the peak can be determined, it should be possible to estimate the amount of mass in the shell by looking at the peak luminosity and the shape of the hardness ratio versus time. As usual in astronomy this can only be done if the distance to the source is known; however, in this model at least there is an upper limit on the luminosity the model can tolerate, and thus on the distance for a given flux.

When we consider repetitive sources on this model, we must strongly distinguish between the two limiting cases. In the gravitational limit the transfer of energy to and from the thermonuclear source is independent of the accretion rate; the increase in compression energy is very small since the accreted mass is small compared to the mass in the shell. The period differs from that of an imaginary perfectly elastic ball only to the extent that the burning phase takes a small but finite amount of time. In the QSP limit, however, the energy returned by the shell never exceeds forty percent of the initial shell energy. The period thus depends on the efficiency of the recompression process after the shell returns to the surface. The energy for the next outburst must be supplied by the matter accreted during the cycle; it cannot be stored in the shell. Even more striking is the fact that the QSP period depends on the shell mass, while the gravitational one does not.

In attempting to apply the model to known pulsed sources we immediately have a problem in isolating the source characteristics in which we are interested. The pulsating x-ray sources are so rich in their behavioral phenomena, that a model this simplified cannot hope to account for all of them. Her X-1, for example, has a highly variable pulse shape which shows some signs of the characteristic decline in hardness ratio. However, since many pulses are integrated to get the published shapes, and these time averaged shapes also vary in time, it is not possible to rigorously check the spectrum evolution against the shape of the pulse. The stellar mass associated with this source is rather high, $\sim 1.2\ M_\odot$. This argues for the gravity dominated regime, unless the mass in the shell is taken to be extremely low. The overall period stability seems to indicate this regime as well, since if the changes in pulse shape are attributed to lumpiness in the accreting gas, one would expect this to show up as jitter in the period of a QSP source. Since the period goes as $\frac{1}{\rho}$ and the luminosity goes as ρ, changes in the density should produce comparable fractional changes in both period and luminosity. The observed hardness ratios are around 1.1 with a low energy cutoff. Subject to the problems mentioned above, this is consistent with a peak temperature of ~ 2 x 10^8 K. The period and spectrum are then both consistent with an almost purely gravitational equation of motion if the stellar radius exceeds the classical cold white dwarf value for its mass by as much as 20 percent. On the other hand, the indicated distance to this source seems to be at least 2 Kpc (Forman et al. 1972), in which case the luminosity would exceed the opacity limit derived in Chapter II.

Strictly on the basis of pulse shape and spectral behavior, the most intriguing similarity between the model predictions and an observed source is the case of the burst sources. These seem to display a pulse decay which is often fitted to an exponential, but which in at least one case exceeds the fitted function at the peak (Clark et al. 1976), reminiscent of the QSP cases. This same burst has been analyzed in terms of its hardness ratio. Although the data is somewhat inconclusive, the hardness ratio seems to increase rather sharply, followed by a leveling off or slow decrease. This has been interpreted as evidence for reprocessing in a surrounding medium. However, the rise in hardness ratio seems to be associated with a time lag between the peaks in the two energy bands, while the ratio is flat or declining throughout the decay phase. The indicated spectrum is appropriate for temperatures less than or the order of 2 x 10^8 K, with some absorption at low energies.

One speculation as to a model for such a burst is that both of the acceleration mechanisms are operative here. Thus the shell is initially accelerated by radiation pressure, prior to the generation and arrival of the detonation shock. A problem with this interpretation is that there is some evidence for a decline in the low energy band prior to or coincident with the high energy peak. If this is real it would seem to argue against a velocity effect with a purely thermal spectrum, and require some sort of processing of the spectrum. The high energy band does seem to decay somewhat faster than the low energy band, as expected for a velocity variation and thermal emission.

Looking at the overall source characteristics, of course, one is hard put to reconcile this model with the suggested association of the burst sources with globular clusters. Not only is the simple association difficult to understand, but the implied distances put the luminosities well above the opacity limits for white dwarfs.

Another, recently discovered, class of sources with certain similarities to the models in the QSP regime is that of the repetitive burst sources (Lewin et al. 1976, Clark et al. 1976). Although the observations are not yet adequate to attempt a detailed model fit, the bursts show the quasi-exponential tails seen in the QSP profiles. In at least some cases the timing of the bursts is quasi-periodic, with a good deal of jitter. One possibility for this behavior is that of a model in the QSP regime, and in which the depth of the burning layer, and thus the initial shell mass, is somewhat variable.

Of particular interest is the so-called multiburster, MXB 1730-335, discovered by Lewin et al. (1976). In this source the interval following a burst seems to be directly proportional to the total energy in the burst, while the peak intensity of the burst remains nearly constant. Clark (1976) has observed that this is suggestive of a relaxation oscillator in which some energy reservoir is emptied by varying amounts in the bursts, and must be refilled to some critical level before the next burst can occur. Since the shell in the QSP model returns at most forty percent of its initial energy, the larger the initial shell energy, the longer the necessary compression period to replace the energy lost. Thus if for some reason the initial shell mass is variable but the velocity is much less so, we would expect behavior similar to that which is observed. It remains to be determined whether the bursts display the necessary spectral evolution, and the nature of the process which would be necessary to modulate the burning depth remains entirely conjectural.

Finally, we need to consider the possible effects of relaxing some of the overall model assumptions, in particular the assumed form of the accretion flow. In any real source there is quite probably an accretion disk rather than a simple radial infall. It is thus quite conceivable that the gas accretes to the surface at less than the free fall velocity. For a given set of model process becomes a competitive loss mechanism. Because Katz and Salpeter assumed the maximum conceivable burning rate in computing their limits, Guthrie and Tademaru (1975) developed a more general expression for the ratio of the inverse Compton (IC) to free-free (FF) loss rates in an ionized gas at given temperature and density as a function of the radiation temperature, T_R, of the underlying black body surface. This expression for the loss ratio, R_L, is

$$R_L \simeq .6 \times 10^{-11} T_R^4 \frac{T_e^{1/2}}{N_e}$$

where T_e and N_e are the electron temperature and number density (cm^{-3}) respectively. Figure 7-1 shows this relationship for various values of the electron parameters. It should be noted that if free-free losses are the dominant process at the shock itself, they dominate throughout the region, since $T_e^{1/2}/N_e$ decreases rapidly as the gas flows away from the shock. If IC cooling is important at all it will be important at the peak of the outburst, raising the possibility that a "critical" case, $R_L \simeq 1$, could produce the dips sometimes observed in x-ray pulses, particularly in Her X-1. However, if the shell temperatures exceed the values of a few times 10^5 indicated by the calculations in S4, the characteristic photon energies may be degraded below the interstellar opacity cutoff. In that case these sources would be very difficult to detect.

A last possibility not considered in this work is modification of the accretion flow by the x-ray emission itself. This was considered in the case of a standing shock by DeGregoria and Woltjer parameters this will tend to flatten the decay slope and broaden the outburst. It will also lower the temperatures involved for a given ejection velocity, although this will be negligible if the ejection velocity is large compared to the accretion velocity. More significantly, it would lower the maximum allowed luminosity for a given source by increasing the necessary density, and thus the opacity, for a given rate of energy input.

Another possible consequence of disk accretion is that the density distribution may not be spherically symmetric. The burning shell should still be nearly symmetric, since any significant horizontal temperature gradients will damp the development of the detonation until the layer relaxes. The ejected shell, however, will not remain spherical and plane parallel unless it is in the extreme gravitational limit. This would tend to broaden the peak and flatten the slope of the hardness ratio, since one would then have a distribution of velocities. If the density distribution is highly asymmetric, it could conceivably smear out the peaks completely. This would probably result in heating the outer layers of the star until the matter burned on the surface, since the incoming energy could no longer be efficiently radiated away.

A basic assumption throughout this work has been that the important cooling mechanism in the shocked gas is free-free emission. This has been questioned by Katz and Salpeter (1974), who point out that if the temperature of the optically thick surface below the x-ray emitting region is sufficiently high, the inverse Compton

Figure 7-1: Loss ratio R_L as a function of radiation temperature for various plasma conditions.

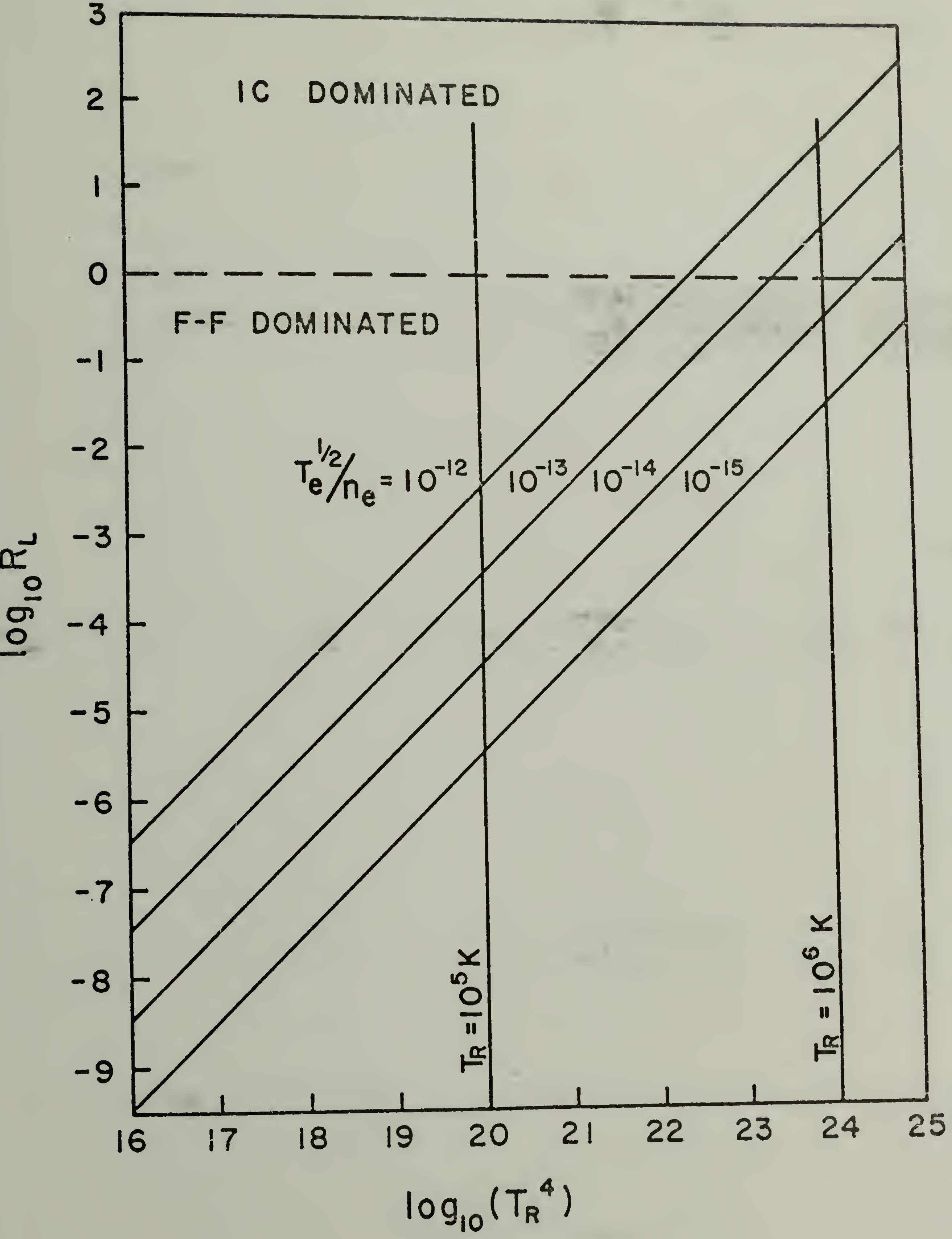
IC DOMINATED
F-F DOMINATED
$T_e^{1/2}/n_e = 10^{-12}$
10^{-13}
10^{-14}
10^{-15}
$T_R = 10^5$ K
$T_R = 10^6$ K
3
2
1
0
-1
-2
-3
-4
-5
-6
-7
-8
-9
$\log_{10} R_L$
16
17
18
19
20
21
22
23
24
25
$\log_{10}(T_R{}^4)$

(1973) and DeGregoria (1974). They found no stable steady state modulation of the emission, but for the ejected shell models this process could conceivably modify the behavior of a given burst to a very large degree.

While this work has been primarily concerned with the development of specific model predictions, I would like to emphasize a point which follows from the most basic and general considerations of this dissertation. Very simply, given that we know of binary systems containing white dwarfs, and that the evolution of these systems must include a mass-transfer phase, there must be some white dwarfs which are compact x-ray sources. The possible temperal behavior of such a source is bounded by the standing-shock models, such as those of Aizu (1973) and Fabian et al. (1976); and by the nova models (e.g. Starrfield and coworkers) which eject nearly the entire non-degenerate shell of the star and cannot repeat until the outer layers have been replaced by accretion. Whether or not there is modulation of the emission due to motion of the surface, a white dwarf in an accretion flow must be a source of x-rays. This is an unavoidable consequence of the depth of the potential well, barring opacity limitations.

The models presented here are an intermediate possibility lying between the bounding behaviors mentioned above. We have shown that repetitive burst emissions and even periodic pulsed emissions are both energetically and dynamically feasible. Although these basic models may eventually be refined and matched with currently known x-ray sources, I would suggest that they are not limited to this approach. Something like them should exist and the characteristic time behavior of the spectrum should make them identifiable in future surveys.

REFERENCES

Aizu, K. 1973, Progr. Theor. Phys., 49, 1184.

Arons, J. 1973, Ap. J., 184, 539.

Axel, L., and Perkins, F. 1971, Ap. J., 163, 29.

Basko, M.M., and Sunyaev, R.A. 1973, Ap. and Space Sci., 23, 117.

Blumenthal, G.R., Cavaliere, A., Rose, W.K., and Tucker, W.H. 1971, Ap. J., 163, 29.

Blumenthal, G.R , and Tucker, W.H. 1974, in X-Ray Astronomy, Ap. and Space Sci. Libr. V. 43, ed. R. Giacconi, and H. Gursky (Dordrecht; Boston: D. Reidel).

Cameron, A.G.W. 1966, Nature, 212, 493.

Cameron, A.G.W. 1975, Ap. and Space Sci., 32, 215.

Canizaves, C.R. 1976, Ap. J., 207, L101.

Clark, G.W., Jernigan, J.G., Bradt, H., Canizaves, C., Lewin, W.H.G., Li, F.K., Mayer, W., McClintock, J., and Schnopper, H. 1976, Ap. J., 207, L105.

DeGregoria, A. 1974, Ap. J., 189, 555.

DeGregoria, A., and Woltjer, L. 1973, Nature Phys. Sci., 246, 108.

Doxsey, R., Bradt, H.V., Levine, A., Murthy, G.T., Rappaport, S., and Spada, G. 1973, Ap. J., 182, L25.

Fabian, A.C., Pringle, J.E., and Rees, M. 1976, M.N.R.A.S., 175, 43.

Forman, W., Jones, C.A., and Liller, W. 1972, Ap. J., 177, L103.

Guthrie, P.D., and Tademaru, E.H. 1975, Ap. J., 201, 415.

Katz, J.I., and Salpeter, E.E. 1974, Ap. J., 193, 429.

Lasker, B. 1965, Ap. J., 143, 700.

Lewin, W.H.G., Doty, J., Clark, G.W., Rappaport, S.A., Bradt, H.V.D., Doxsey, R., Hearn, D.R., Hoffman, J.A., Jernigan, J.G., Li, F.K., Mayer, W., McClintock, J., Primini, F., and Richardson, J. 1976, Ap. J., 207, L95.

Liller, M.H., and Liller, W. 1976, Ap. J., 207, L109.

Mestel, L. 1952, M.N.R.A.S., 117, 598.

Prendergast, K., and Burbidge, G. 1968, Ap. J., 151, L83.

Pringle, J.E., and Rees, M.J. 1972, Astron. and Ap., 21, 1.

Richtmyer, R.D. 1957, Difference Methods for Initial Value Problems (New York: Interscience).

Rose, W.K. 1968, Ap. J., 152, 245.

Schwarzschild, M. 1958, Structure and Evolution of the Stars (Princeton, Princeton University Press).

Spitzer, L. 1956, Physics of Fully Ionized Gases (New York: Interscience).

Spitzer, L. 1962, Diffuse Matter in Space (New York: Interscience).

Starrfield, S. 1971, M.N.R.A.S., 155, 129.

Starrfield, S., and Truran, J.W., Sparks, W.M., and Kutter, G.S. 1972, M.N.R.A.S., 176, 169.

Starrfield, S., Sparkes, W.M., and Truran, J.W. 1974a, Ap. J., 192, 647.

Starrfield, S., Sparkes, W.M., and Truran, J.W. 1974b, Ap. J., 192, 817.

Strittmatter, P.A., Brecher, K., Burbidge, G.R. 1972, Ap. J., 174, 91.

Yokoo, H., and Hoshi, R. 1974, Progr. of Theor. Phys., 51, 418.

Zel'dovich, Ya., B., and Raizer, Yu., P. 1966, Physics of Shock Waves and High Temperature Phenomena (New York: Academic Press).